CPUE standardization of swordfish (*Xiphias gladius*) caught by Taiwanese large-scale longline fishery in the Indian Ocean

Chih-Yu Lin, Sheng-Ping Wang*, Wen-Qi Xu

Department of Environmental Biology and Fisheries Science, National Taiwan Ocean University, Keelung, Taiwan.
* Corresponding author: wsp@mail.ntou.edu.tw

ABSTRACT

This paper briefly describes historical patterns of swordfish catches caught by Taiwanese large-scale longline fishery in the Indian Ocean. The cluster analysis was adopted to explore the targeting of fishing operations. In addition, the delta-inverse Gaussian generalized linear models were selected to conduct the CPUE standardizations of swordfish caught by Taiwanese large-scale longline fishery. The results indicate that the catch rates of the positive catches and the opportunity of catching swordfish might be determined by the position of fishing operations in areas other than Area SW and might be influenced by the targeting of the fishing operation in Area SW. The standardized CPUE series revealed different trends by areas, they slightly decreased in northern areas (NW and NE) and increased in southern area (SW and SE) in recent years.

1. INTRODUCTION

In the past, swordfish (*Xiphias gladius*) was mainly caught by the longline fisheries from Taiwan, Japan, Spain and Indonesia. Since large-scale drift gillnets had been completely prohibited in the high seas in 1993, currently, only few countries, including Sri Lanka, continued to use drift gillnets to catch swordfish in their territorial waters. In recent year, offshore longline catches, including sharks and swordfish-targeted longlines, accounted for 53.9% of total swordfish catches in the Indian Ocean, followed by line (30.2%) and gillnet (14.9%). The remaining catches taken with other gears contributed to 1% of the total catches (IOTC, 2022a; 2022b).

After 1990, catches of swordfish increased sharply as a result of changes in targeting from tunas to swordfish by part of the Taiwanese longline fleet, along with the development of longline fisheries in Australia, France (La Réunion), Seychelles and Mauritius and arrival of EU longline fleets and other fleets from the Atlantic

Ocean. Since the mid-2000s annual catches have fallen steadily, largely due to the decline in the number of Taiwanese longline vessels active in the Indian Ocean in response to the threat of piracy; however since 2012 catches appear to show signs of recovery as a consequence of improvements in security in the area off Somalia. In recent years, swordfish catches were mainly made by Sri Lankan longline-gillnet fleet (25%), Taiwanese longline fleet (21%), India coastal longline fleet (9%) and swordfish-targeted longline of EU, Spain (9%) (IOTC, 2022a; 2022b).

IOTC conducted a stock assessment for swordfish in the Indian Ocean in 2020 and the results indicated that the stock was not overfished and not overfishing and the recent catches were below the MSY level. However, the Southern regions exhibited declining biomass trends which indicated higher depletion in these regions (IOTC, 2022a; 2022b). Therefore, this study conducted CPUE standardization for swordfish in the Indian Ocean for providing the relative abundance indices for further stock assessment.

2. MATERIALS AND METHODS

2.1. Catch and Effort data

In this study, daily operational catch and effort data (logbook) with 5x5 degree longitude and latitude grid for Taiwanese longline fishery during 1979-2022 were provided by Oversea Fisheries Development Council of Taiwan (OFDC). For the area stratification, this study adopted the four areas stratification for swordfish by Wang and Nishida (2011) (Fig. 1).

As the discussions and suggestions from previous IOTC meetings (2021a; 2021b), Taiwanese data before 2005 were recommended not using to analyze the targeting of fishing operations and conduct the CPUE standardization for tropical tuna due to the problem of data quality. However, the data problem might not only influence the misreport for the catches of major tropical tunas but also lead to uncertainties in the catch and effort data for other species. Therefore, CPUE standardizations were conducted using the data from 2005 to 2022 as suggested in previous meetings.

2.2. Cluster analysis

The details of the procedures of cluster analysis were described in Wang et al. (2021). This study adopted a direct hierarchical clustering with agglomerative algorithm, which brings a fast and efficient implementation through features of memory-saving routines in hierarchical clustering of vector data (Müllner, 2013). The

trials conducted using R function “hculst.vector” of package “fastcluster” (Müllner 2021) with Ward's minimum variance linkage methods (“ward.D” for the argument “method” in “hclust.vector” of R function) applied to the squared Euclidean distances between data points calculated based on the species composition.

The number of clusters was selected based the elbow method, i.e. the change in deviance between/within clusters against different numbers of clusters. The number of clusters was determined when the improvement in the sum of within-cluster variations was less than 10%.

2.3. CPUE Standardization

Although Taiwanese longline fishery seasonally targeted swordfish in the southwestern Indian Ocean, a large amount of zero-catches was recorded in the operational catch and effort data sets because swordfish was still mainly the bycatch species of Taiwanese longline fishery in the entire Indian Ocean. Historically, ignoring zero observations or replacing them by a constant was the most common approach. An alternative and popular way to deal with zeros was through the delta approach (Hinton and Maunder, 2004; Maunder and Punt, 2004). IOTC (2016) also noted the use of the delta approach to accommodate the high proportion of zero catches. Therefore, the delta-general linear models with different assumptions of error distribution were applied to conduct the CPUE standardization of swordfish in the Indian Ocean (Pennington, 1983; Lo et. al., 1992; Pennington, 1996; Andrade, 2008; Lauretta et al., 2016; Langley, 2019).

As the approach of Wang (2020), the models were simply conducted with the main effects of year, quarter, longitude, latitude and fishing targeting (clusters), and then the interactions between main effects with significance were incorporated into the models. Hinton and Maunder (2004) indicated that interactions with the year effect would invalidate the year effect as an abundance index. Therefore, the interactions associated with the year effect were not considered in the model. The collinearity diagnostics were also conducted for all of the main effects and interactions using generalized variance-inflation factors (GVIF, Fox and Monette, 1992; Fox and Weisberg, 2019). In this study, the main effects or interactions with the value of $GVIF^{1/2df}$ less than 5 were retained in the model.

CPUE standardizations were also performed by areas separately (Fig. 1). The models for positive catches and delta models were conducted as follows:

For CPUE of positive catches:

$$Catch = \mu + Y + Q + CT + Lon + Lat + T + offset(\log(Hooks)) + \text{interactions} + \varepsilon^{pos}$$

Delta model for presence and absence of catches:

$$PA = \mu + Y + Q + CT + Lon + Lat + T + Hook + \text{interactions} + \varepsilon^{del}$$

where $Catch$ is the catch in in number/1,000 hooks
PA is the presence/absence of catch,
$Hooks$ is the effort of 1,000 hooks,
μ is the intercept,
Y is the effect of year,
Q is the effect of quarter,
CT is the effect of vessel scale,
Lon is the effect of longitude,
Lat is the effect of latitude,
T is the effect of targeting (cluster),
ε^{pos} is the error term assumed based on various distribution,
ε^{del} is the error term, $\varepsilon^{del} \sim$ Binomial distribution.

To examine the appropriateness to the assumption of error distribution, this study applied normal, Poisson, Gamma, negative-binomial, tweedie and inverse Gaussian distributions to the error distribution of the model for the positive catches and specified "log" for the model link function. The stepwise searches ("both" direction, i.e. "backward" and "forward") based on the values of Akaike information criterion (AIC) were performed for selecting the explanatory variables for each model. Then, the coefficient of determination (R^2), and Bayesian information criterion (BIC) were calculated for the models with selected explanatory variables.

The standardized CPUE were calculated based on the estimates of least square means of the interaction between the effects of year and area, and calculated by the product of the standardized CPUE of positive catches and the delta model:

$$DL^{index} = e^{\log(CPUE)} \times \left(\frac{e^{PA}}{1 + e^{PA}} \right)$$

where DL^{index} is the standardized CPUE.

3. RESULTS AND DISCUSSION

3.1. Historical fishing trends

Figs. 2 and 3 show the distribution of catch (numbers) and CPUE of swordfish based on the logbook data of Taiwanese large-scale longline fishery in the Indian Ocean. The catches of swordfish were mainly made in tropical area and the southwest

Indian Ocean. High CPUE mainly occurred in the tropical area and the southwestern Indian Ocean.

The swordfish catches were mainly caught with high effort in northern waters, especially for the Area NW. Although the catches in the northwestern Indian Ocean increased significantly around 2012, the catches substantially decreased in the following years (Fig. 4 and Fig. 5).

3.2. Cluster analysis

Based on the results from the elbow method, 4 clusters were selected for Areas NW, SW and SE, while 5 clusters were selected for Area NE (Figs. 6 and 7). For each area, the species compositions revealed different patterns by clusters (Fig. 8). Swordfish were not major species for all clusters and areas except for Cluster 5 in Area NE contained relatively high proportions of swordfish in Area NE in the mid-2000s.

Fig. 9 show the swordfish catches and efforts by clusters and areas and swordfish catches were contained in different clusters in different periods when different levels of efforts were deployed. Therefore, the data of all clusters were used to conducted the further CPUE standardizations. The annual trends of the proportions of zero catches of swordfish roughly decreased by years for all areas (Fig. 10).

3.3. CPUE standardization

Based on the AIC model selections for the models for positive catches and delta models, all of the effects were statistically significant and remained in the models for all areas. For the models for positive catches, the models with inverse Gaussian error distribution would be the optimal models for all areas based on the values of AIC and BIC although R^2 may not be higher than other models (Table 1). In addition, diagnostic plots for residuals also indicated that the models with inverse Gaussian error distribution (Fig. 11) should be most appropriate than other models because there were less increasing or decreasing trends in the range of predicted values (plots for other models by areas were not shown here but the residuals revealed obvious patterns with predicted values). Therefore, the delta-inverse Gaussian models were selected to produce the standardized CPUE series.

The ANOVA tables for selected models are shown in Table 2. Except for the impact of the effect of *Y*, the effects of *Lat* and/or *Lon* were the most significant variable for both models with positive catches and delta models in areas other than Area SW. In Area SW, the effects of *T* (clusters) provided the most contributions to the explanation of variance of CPUE for both models with positive catches and delta models than other main effects. Thus, the catch rates of the positive catches and the

opportunity of catching swordfish might be determined by the position of fishing operations in areas other than Area SW and might be influenced by the targeting of the fishing operation in Area SW.

The area-specific standardized CPUE series are shown in Fig. 12 and the CPUE series revealed similar trends for all model. The standardized CPUE of positive catches and catch probability obtained from the selected model are shown in Fig. 13 and CPUE of positive catches and catch probability revealed similar trends except for Area SW.

The standardized CPUE series with 95% confidence intervals obtained from the selected model are shown in Fig. 14. The CPUE series in the area NW generally fluctuated without apparent trends. The CPUE series in the NE area gradually decreased before 2011, increased from 2011 to 2019, and decreased again in recent year. The CPUE series in the Area SW increased before 2007, followed by gradually decrease until 2015, and consistently increased after 2016. The CPUE series in Area SE revealed an increasing trend since 2005, a significant decrease in 2012, and an increase after 2013.

REFERENCE

Andrade, H.A., 2008. Using delta-Gamma generalized linear models to standardize catch rates of yellowfin tuna caught by Brazilian bait-boats. ICCAT SCRS/2008/166.

Fox, J., Monette, G., 1992. Generalized collinearity diagnostics. J. Am. Stat. Assoc., 87: 178–183.

Fox, J., Weisberg, S., 2019. An R companion to applied regression, Third Edition. Thousand Oaks CA: Sage.

Hinton, M.G., Maunder, M.N., 2004. Methods for standardizing CPUE and how to select among them. Col. Vol. Sci. Pap. ICCAT, 56: 169-177.

IOTC, 2016. Report of the 14th Session of the IOTC Working Party on Billfish. IOTC-2016-WPB14-R[E].

IOTC, 2021a. Report of the 19th Session of the IOTC Working Party on Billfish. 13–16 September 2021, Microsoft Teams Online. IOTC–2021–WPB19–R[E].

IOTC, 2021b. Report of the 24rd Session of the IOTC Scientific Committee. 6–10 December 2021, online. IOTC–2021–SC24–R[E]_Rev1.

IOTC, 2022a. Report of the 20th Session of the IOTC Working Party on Billfish. 12–15 September 2022, Online. IOTC–2022–WPB20–R[E].

IOTC, 2022b. Report of the 25th Session of the IOTC Scientific Committee. 5–9 December 2021, Seychelles. IOTC–2022–SC25–R[E].

Langley, A.D., 2019. An investigation of the performance of CPUE modelling

approaches – a simulation study. New Zealand Fisheries Assessment Report 2019/57.

Lauretta, M.V., Walter, J.F., Christman, M.C., 2016. Some considerations for CPUE standardization; variance estimation and distributional considerations. ICCAT Collect. Vol. Sci. Pap. ICCAT, 72(9): 2304-2312.

Lo, N.C.H., Jacobson, L.D., Squire, J.L., 1992. Indices of relative abundance from fish spotter data based on delta-lognormal models. Can. J. Fish. Aquat. Sci., 49: 2515-2526.

Maunder, N.M., Punt, A.E., 2004. Standardizing catch and effort data: a review of recent approaches. Fish. Res., 70: 141-159.

Müllner, D., 2013. fastcluster: Fast Hierarchical, Agglomerative Clustering Routines for R and Python. Journal of Statistical Software, 53(9): 1-18.

Müllner, D., 2021. The fastcluster package: User's manual, Version 1.2.3. https://cran.r-project.org/web/packages/fastcluster/vignettes/fastcluster.pdf

Pennington, M., 1983. Efficient estimation of abundance, for fish and plankton surveys. Biometrics, 39: 281-286.

Pennington, M., 1996. Estimating the mean and variance from highly skewed marine data. Can. J. Fish. Aquat. Sci., 94: 498-505.

Wang, S.P., 2020. CPUE standardization of swordfish (*Xiphias gladius*) caught by Taiwanese large scale longline fishery in the Indian Ocean. IOTC–2020–WPB18–15_Rev1.

Wang, S.P., Nishida, T., 2011. CPUE standardization of swordfish (*Xiphias gladius*) caught by Taiwanese longline fishery in the Indian Ocean. IOTC-2011-WPB09-12.

Wang, S.P., Xu, W.Q., Lin, C.Y., Kitakado, T., 2021. Analysis on fishing strategy for target species for Taiwanese large-scale longline fishery in the Indian Ocean. OTC–2021–WPB19–11.

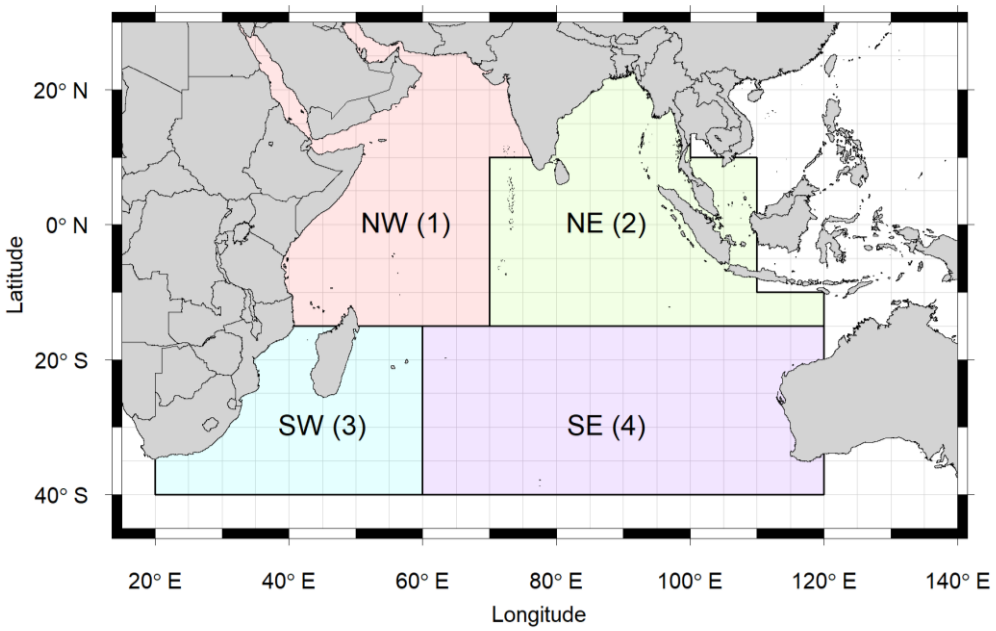

Fig. 1. Area stratification for billfishes in the Indian Ocean.

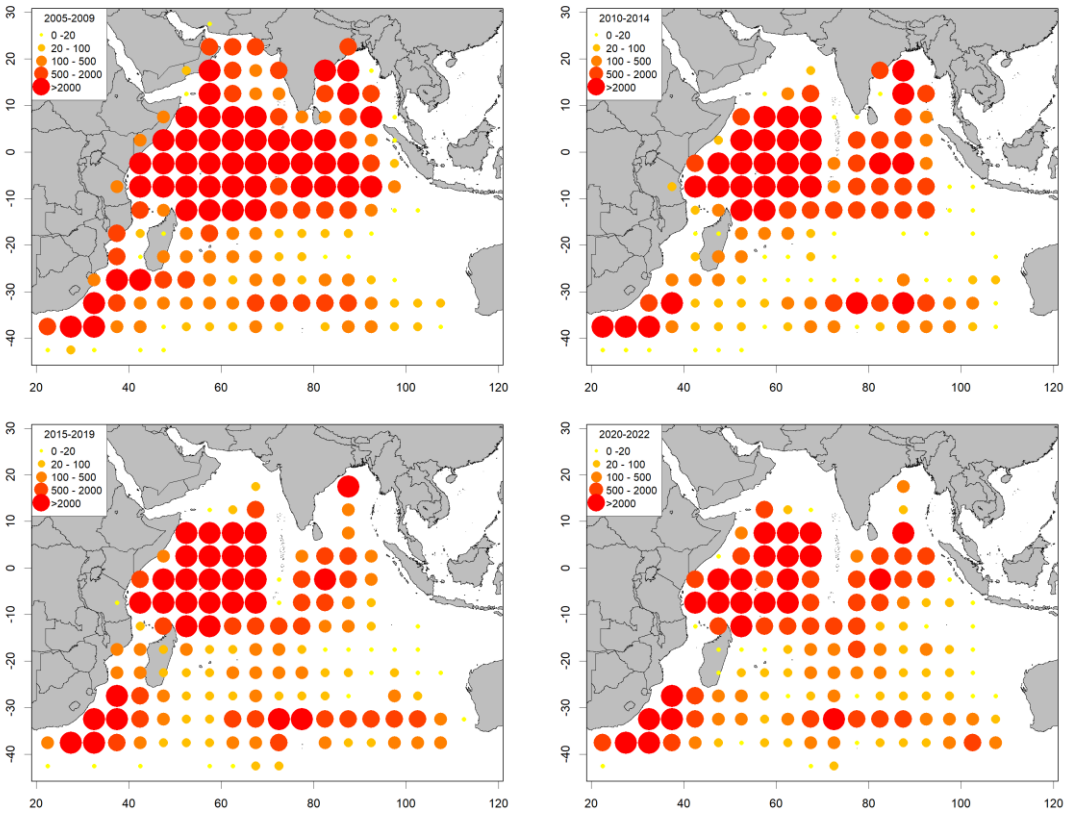

Fig. 2. Swordfish catch distribution of Taiwanese large-scale longline fishery in the Indian Ocean.

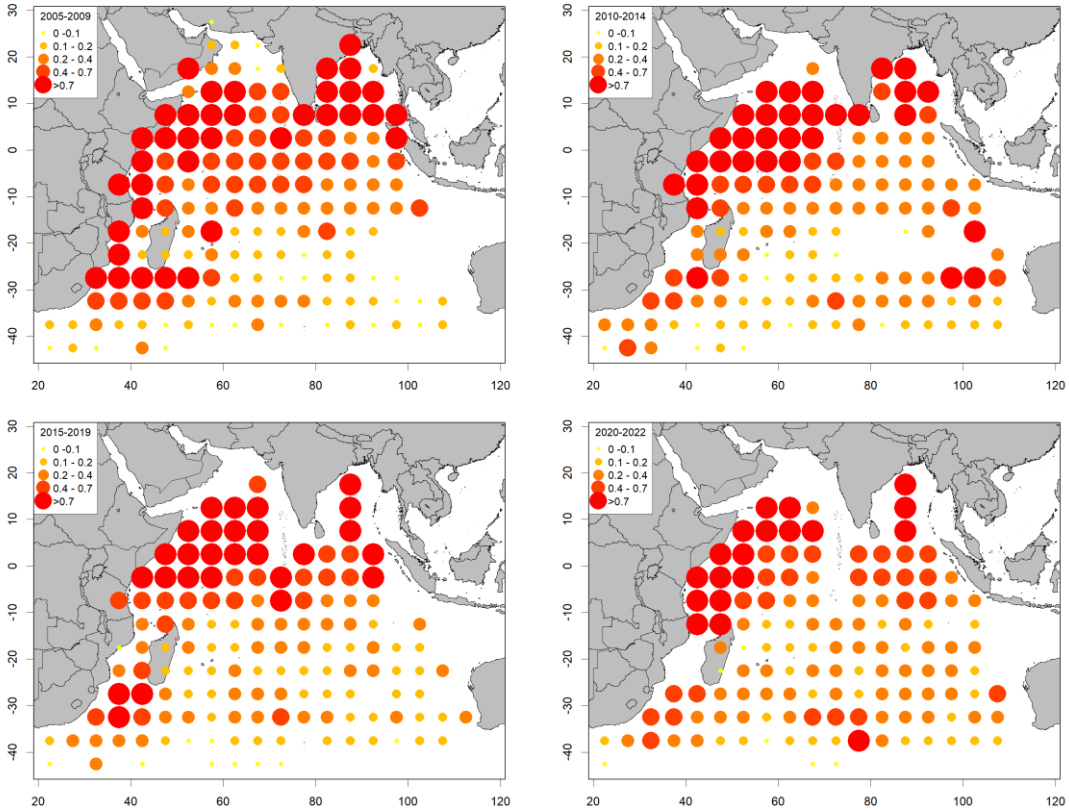

Fig. 3. Swordfish CPUE distribution of Taiwanese large-scale longline fishery in the Indian Ocean.

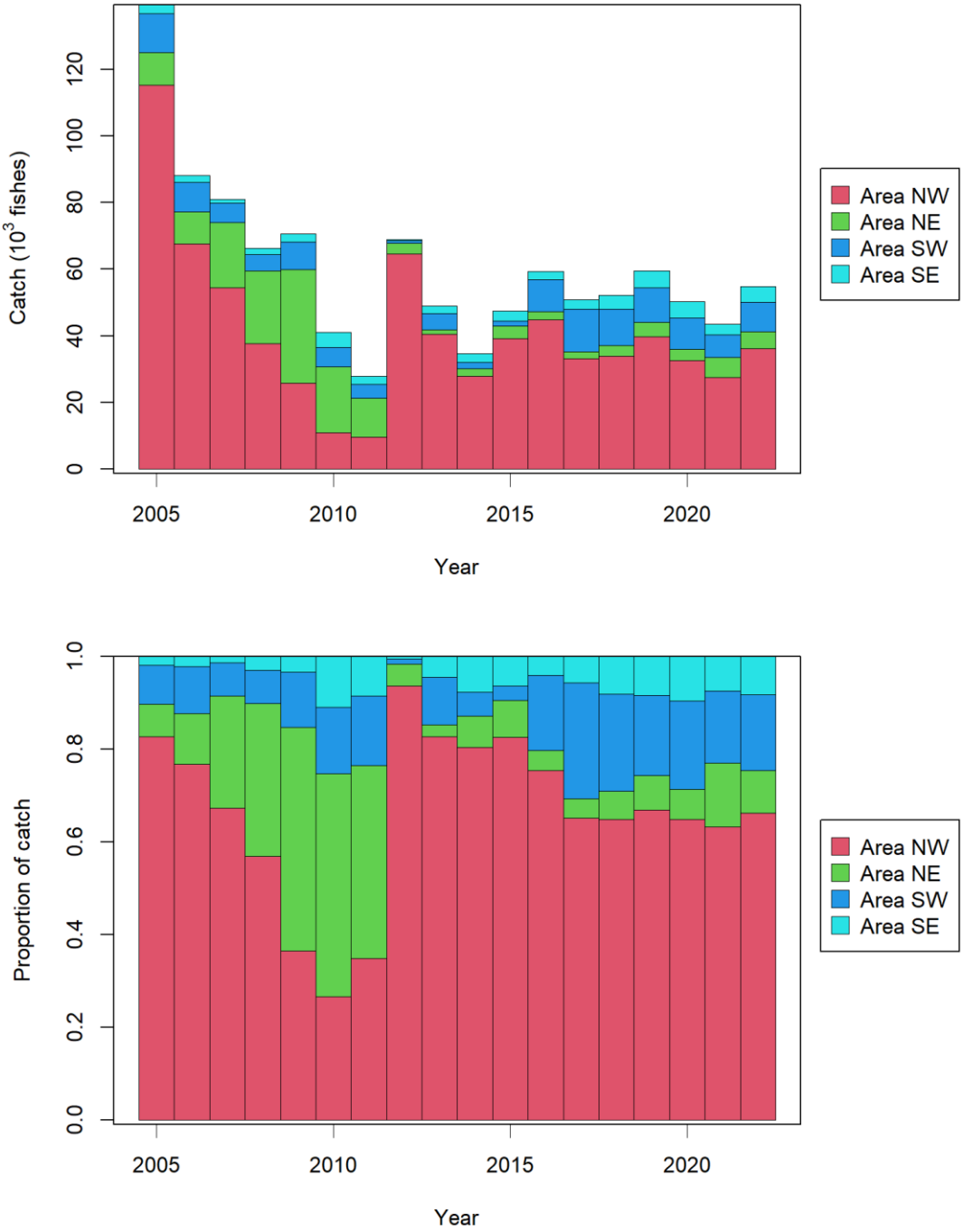

Fig. 4. Annual swordfish catches of Taiwanese large-scale longline fishery in the Indian Ocean.

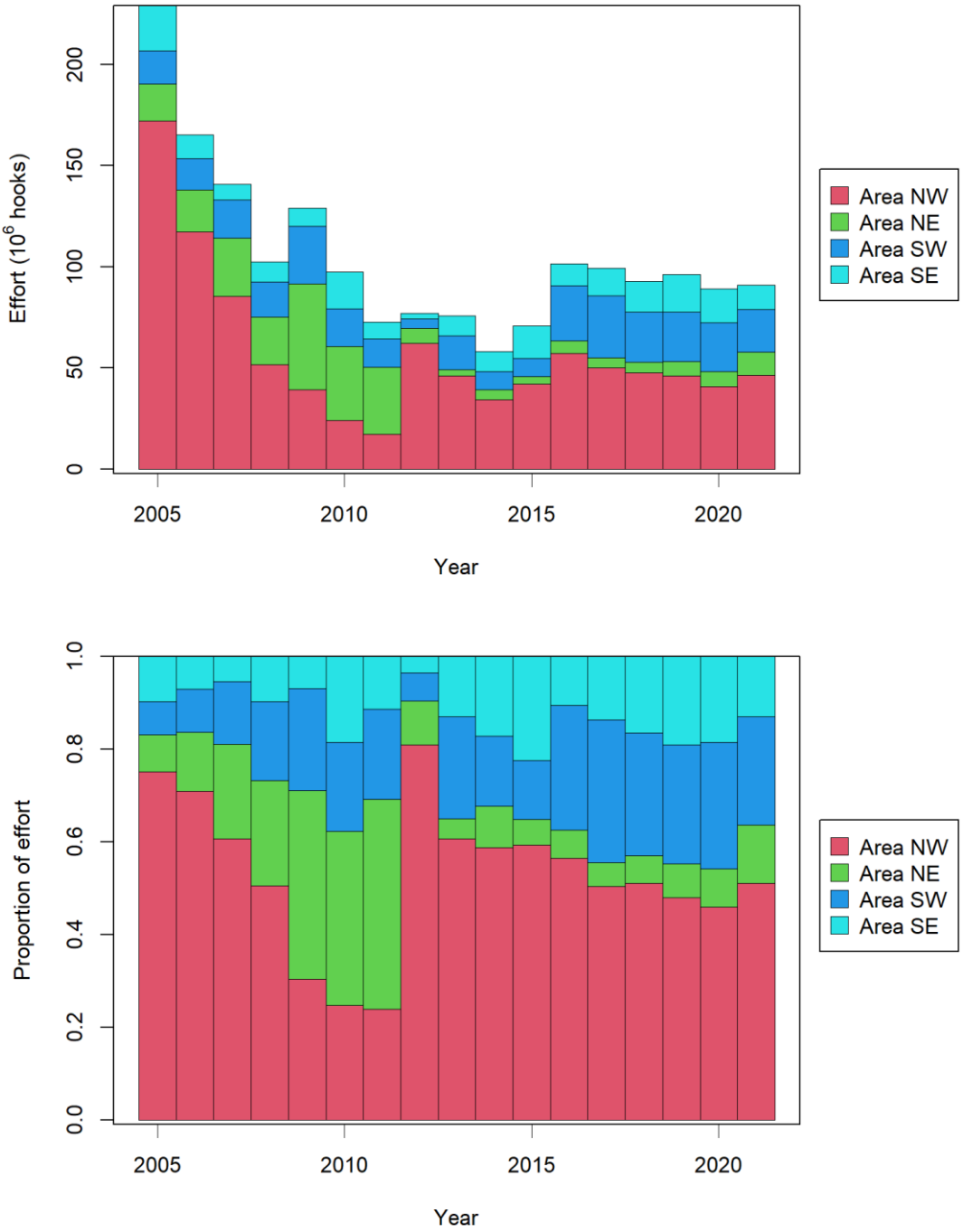

Fig. 5. Annual efforts (number of hooks) of Taiwanese large-scale longline fishery in the Indian Ocean.

Area NW

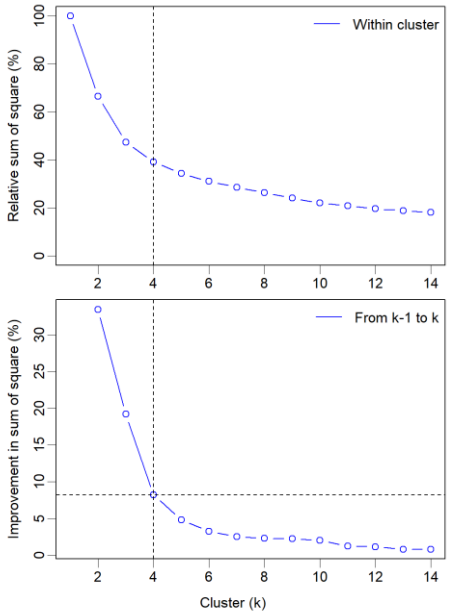

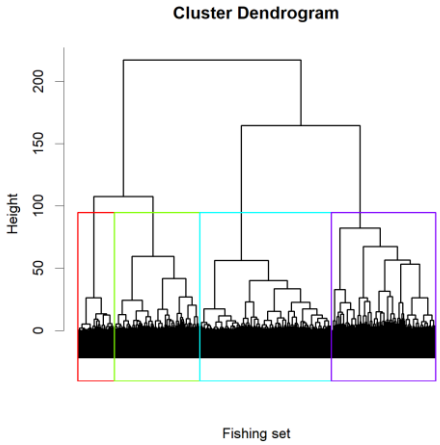

Area NE

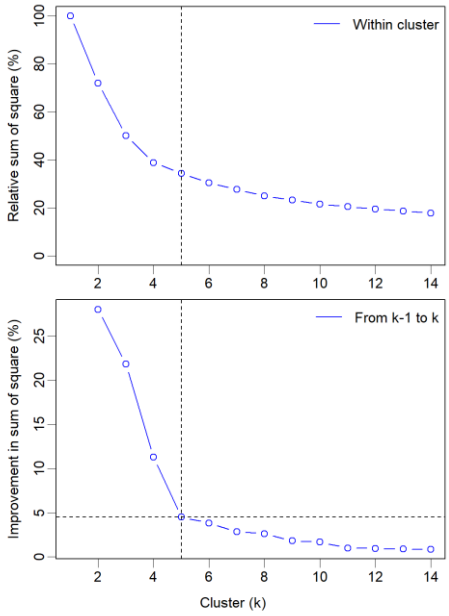

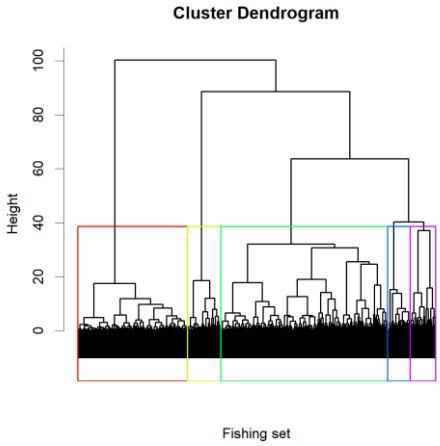

Fig. 6. Sum of squares within clusters for the data of Taiwanese large-scale longline fishery in billfish area of the Indian Ocean.

Area SW

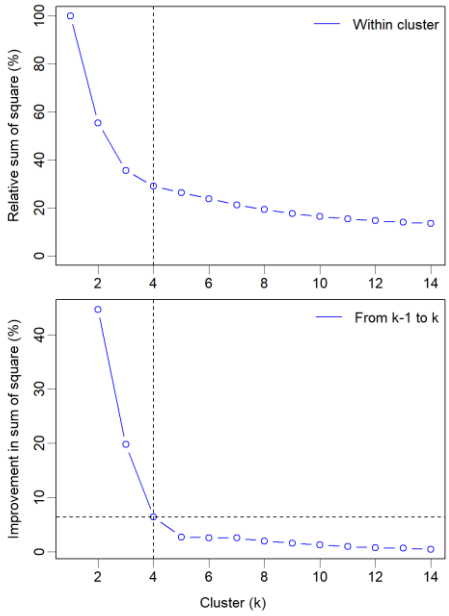

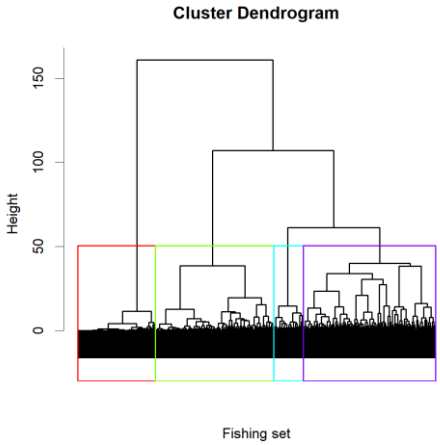

Area SE

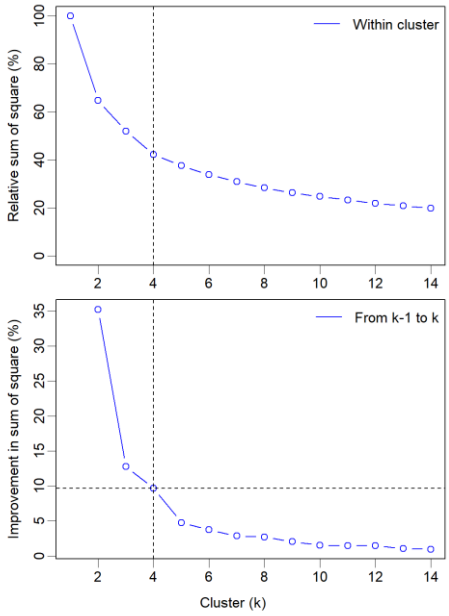

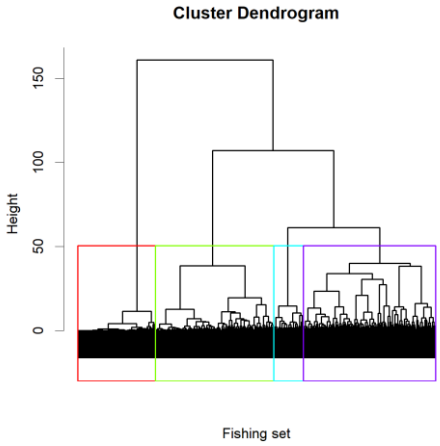

Fig. 6. (continued).

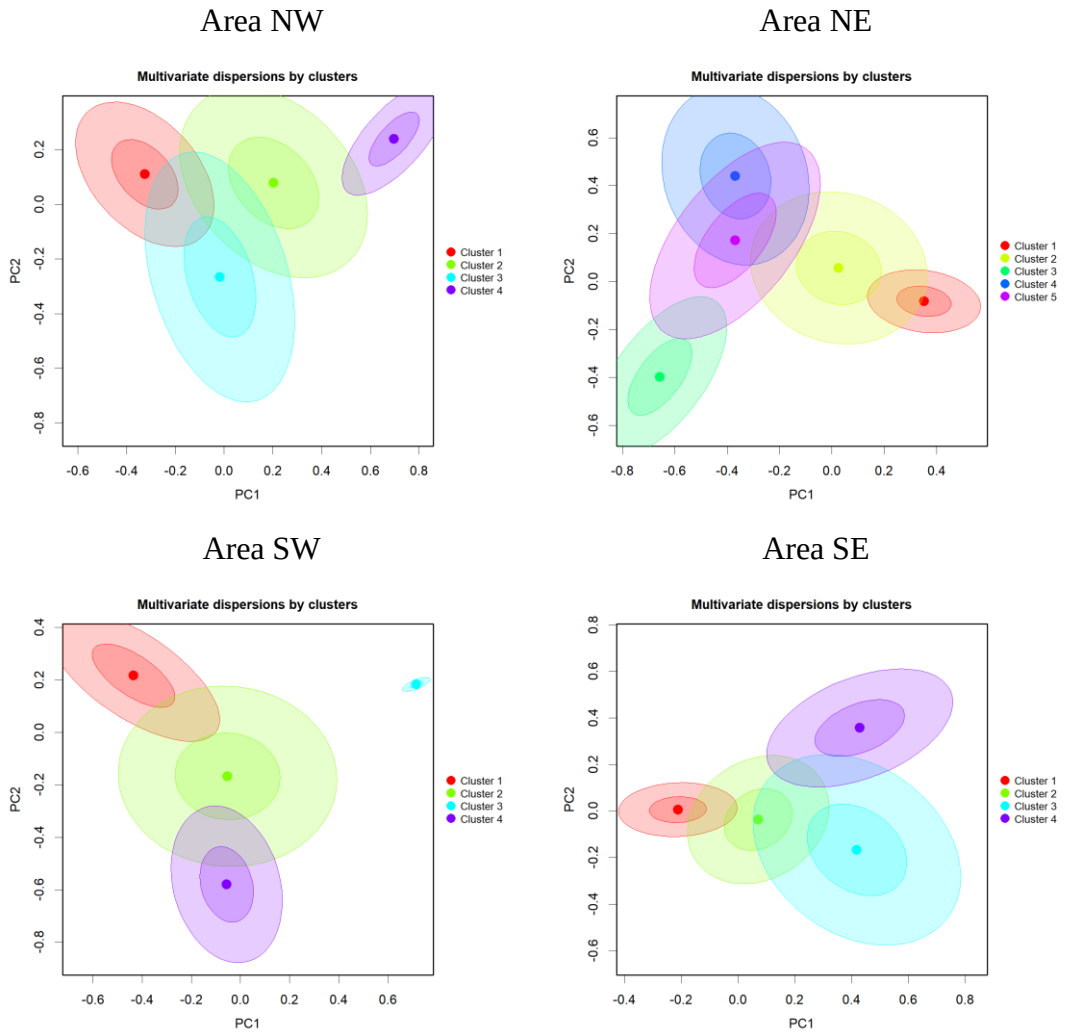

Fig. 7. Multivariate dispersions of the centroids by clusters derived from PCA for the data of Taiwanese large-scale longline fishery in billfish area of the Indian Ocean.

Area NW

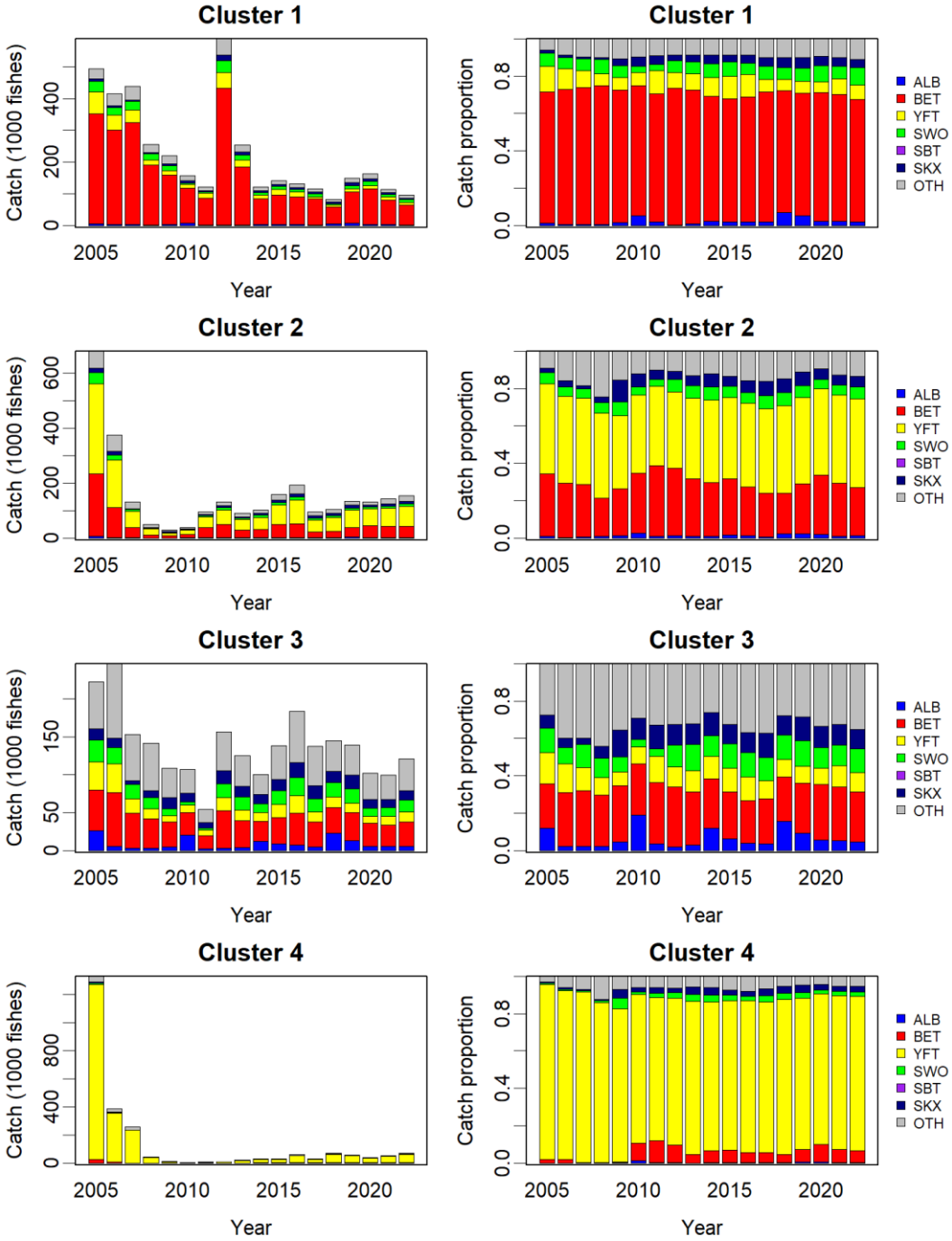

Fig. 8. Annual catches and compositions by species for each cluster of Taiwanese large-scale longline fishery in billfish area of the Indian Ocean.

Area NE

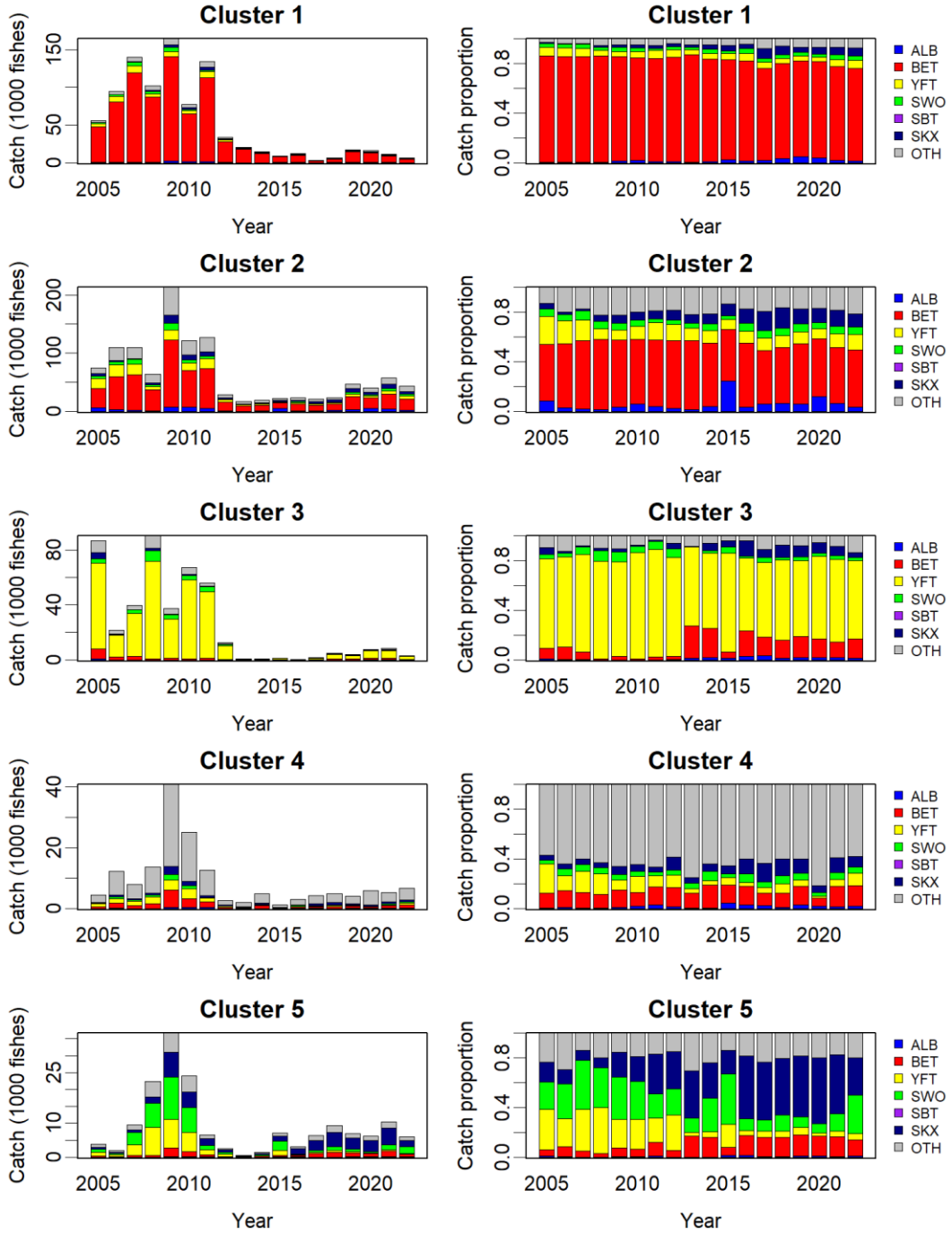

Fig. 8. (continued).

Area SW

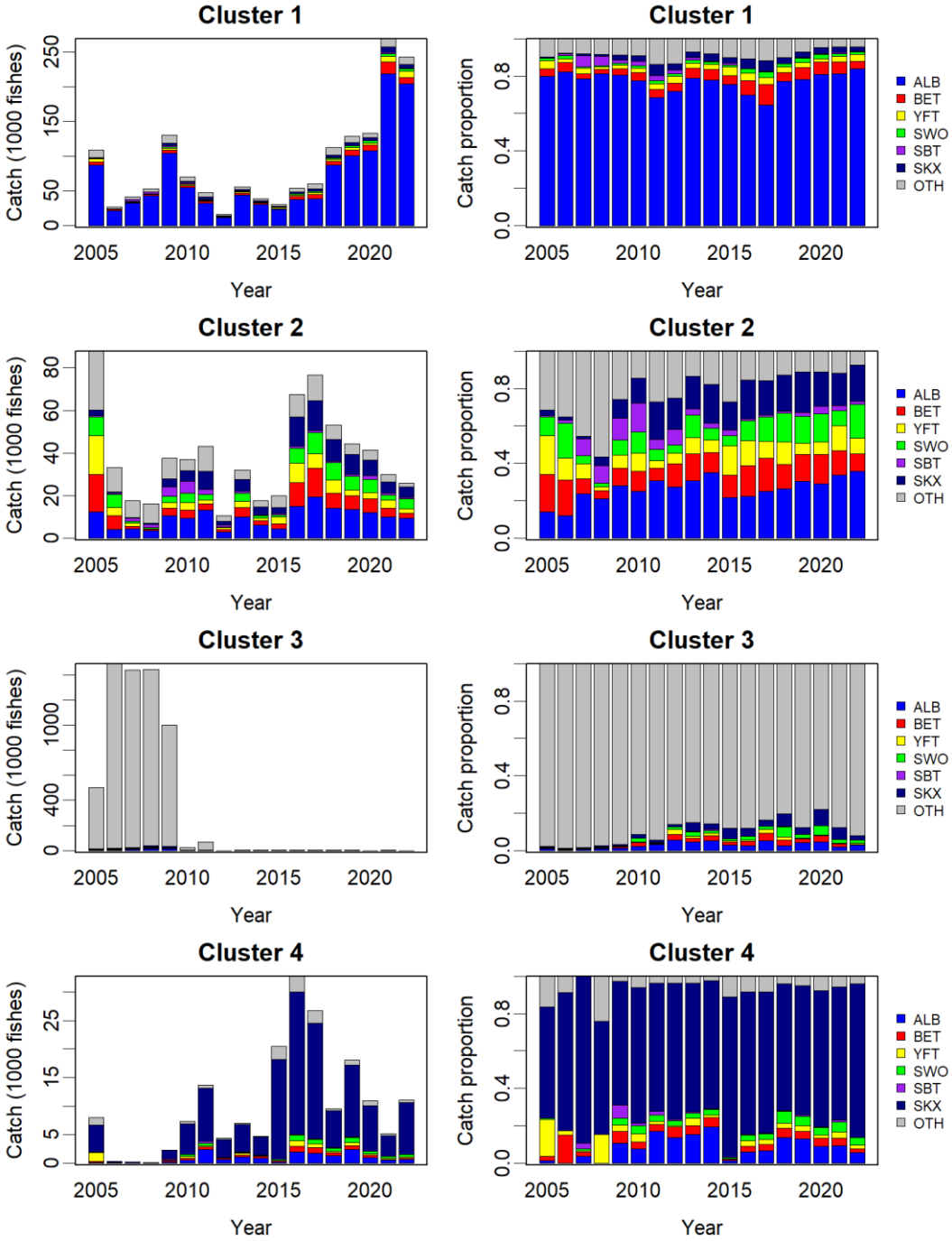

Fig. 8. (continued).

Area SE

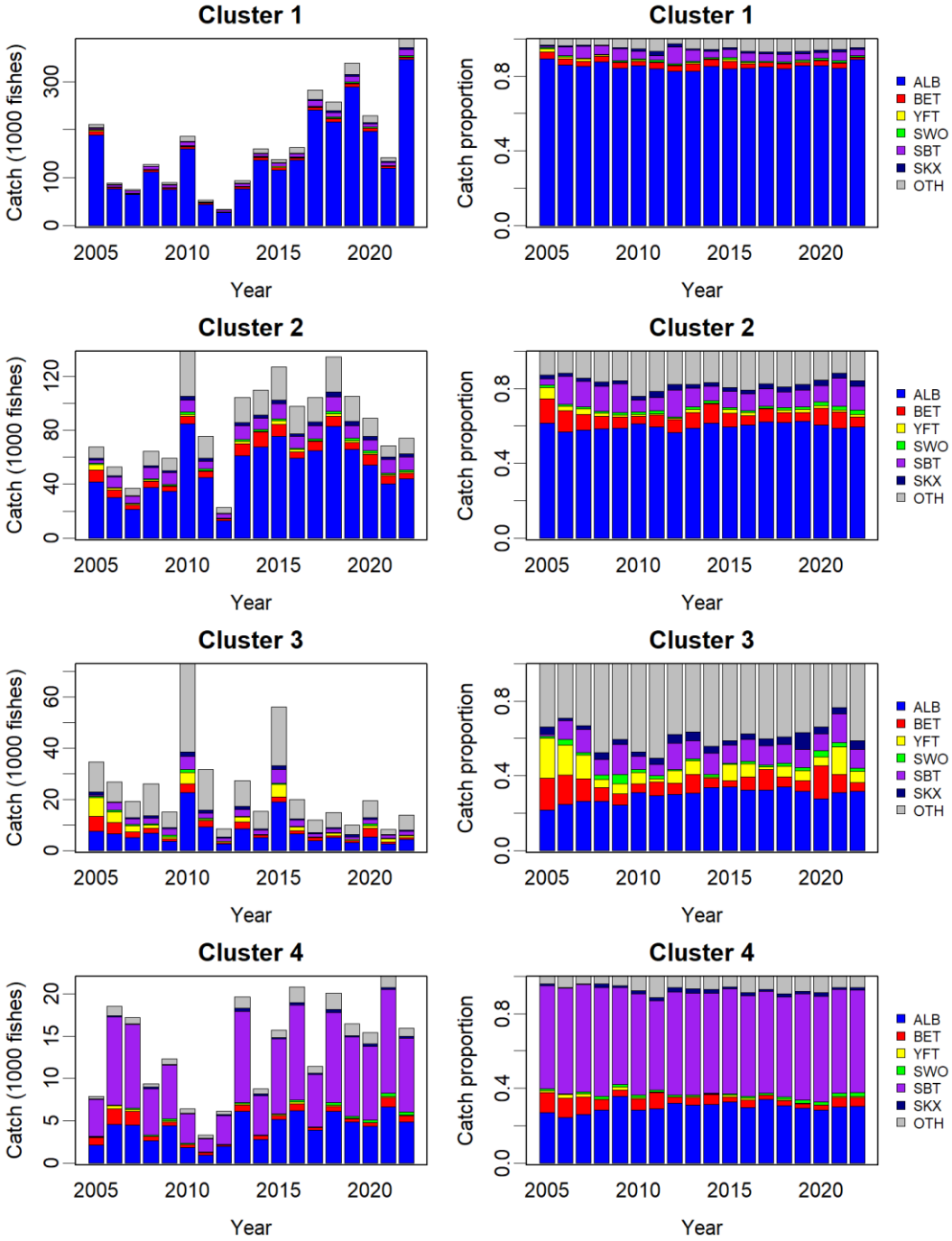

Fig. 8. (continued).

Area NW

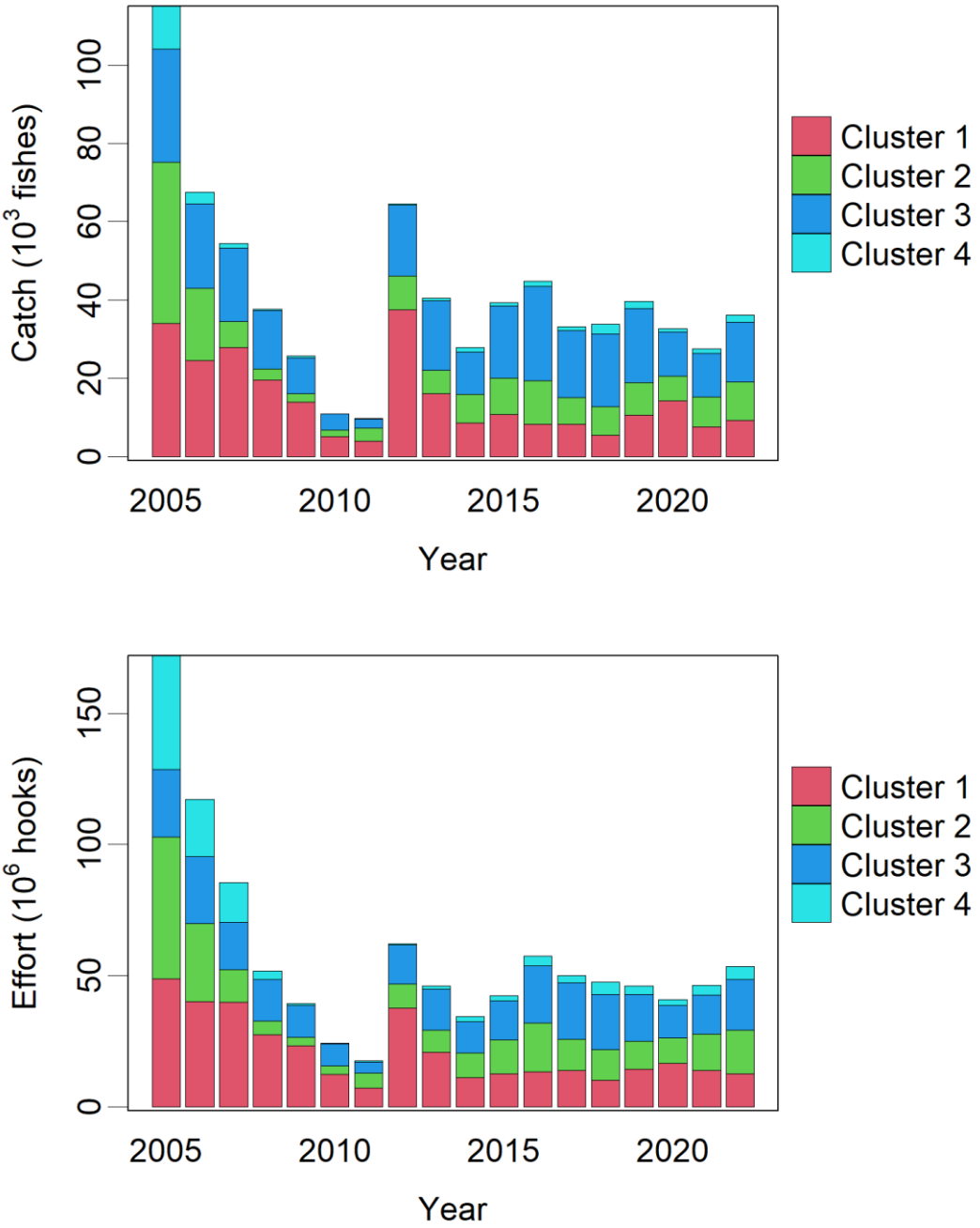

Fig. 9. Annual swordfish catches and efforts for each cluster of Taiwanese large-scale longline fishery in billfish area of the Indian Ocean.

Area NE

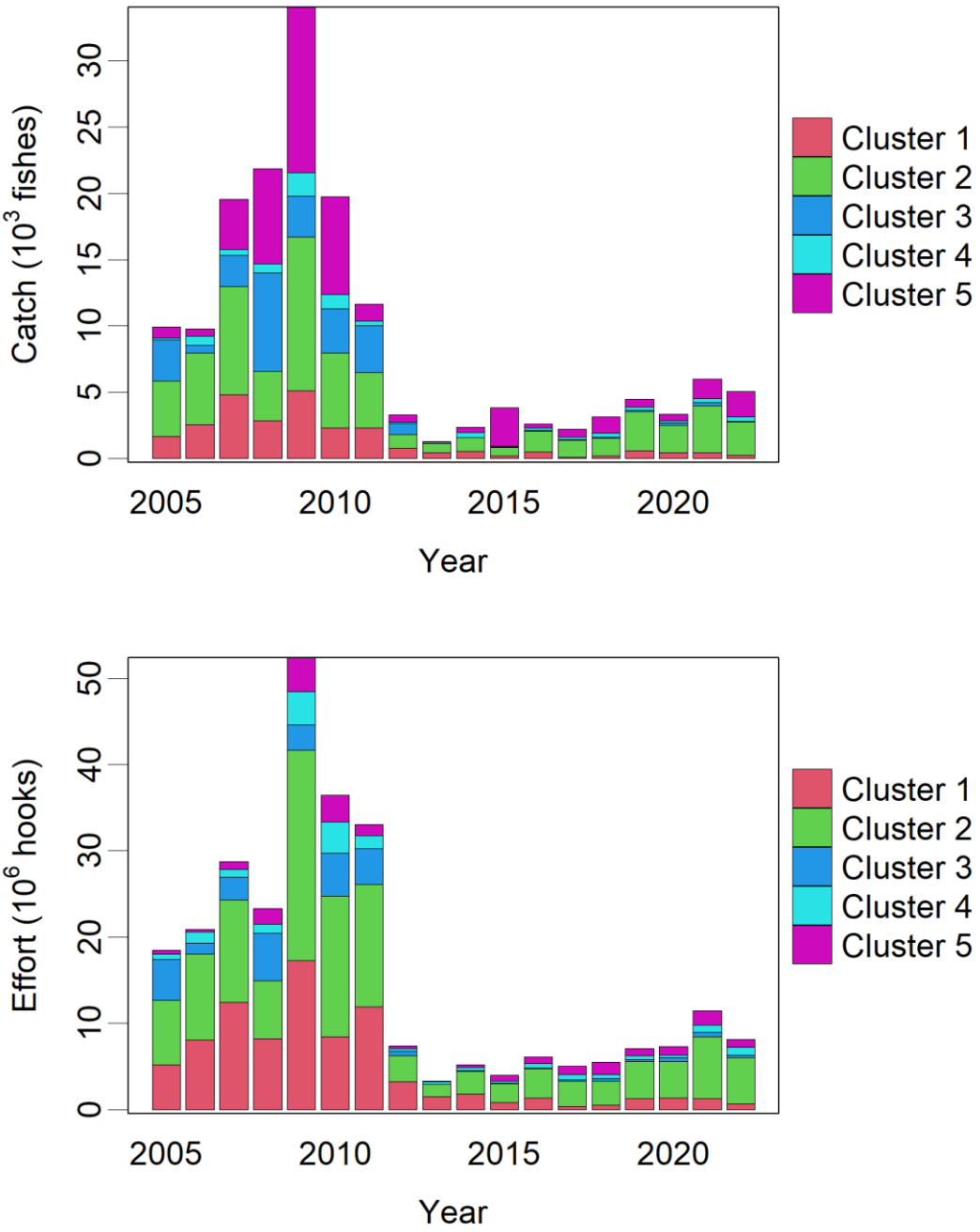

Fig. 9. (continued).

Area SW

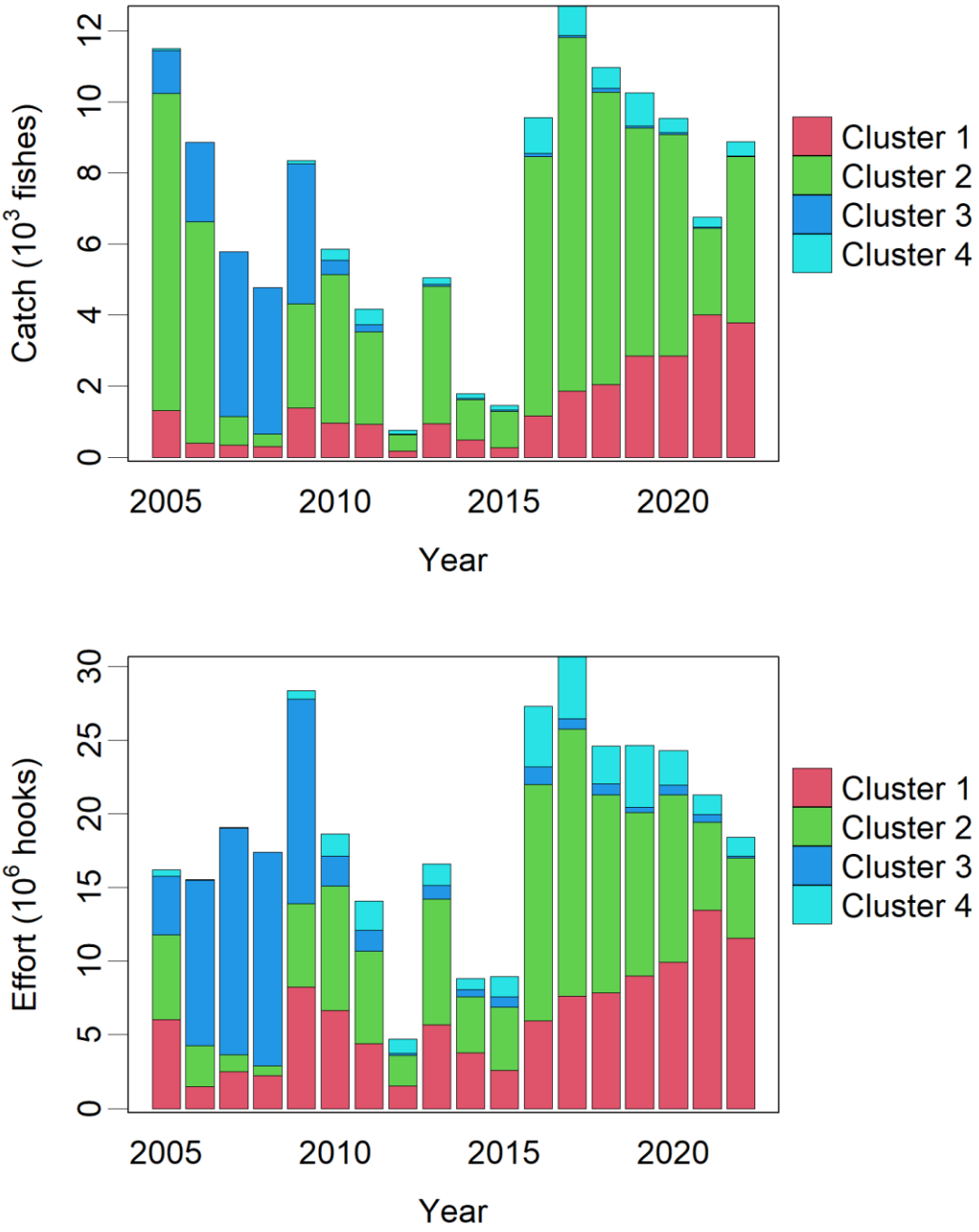

Fig. 9. (continued).

Area SE

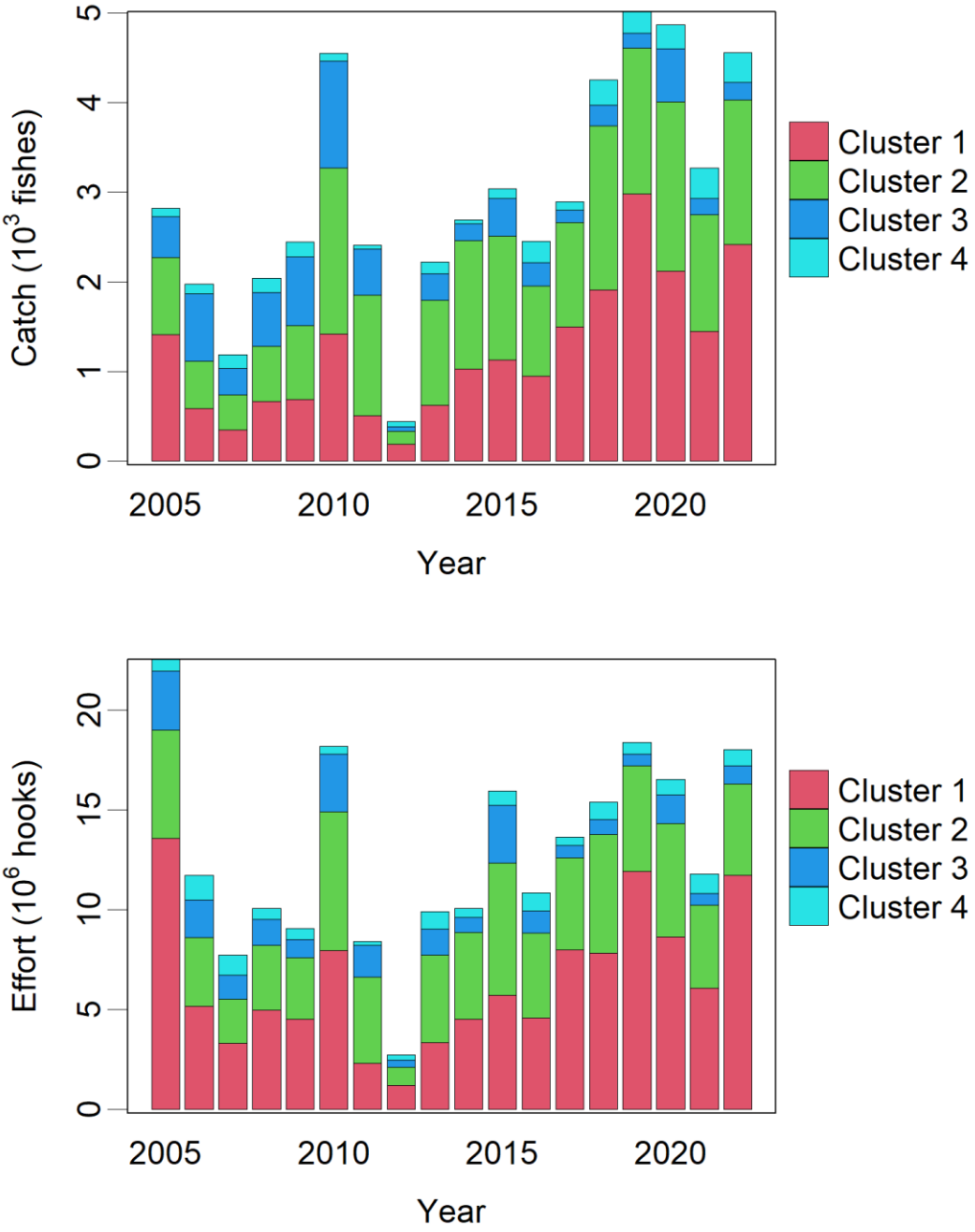

Fig. 9. (continued).

Area NW

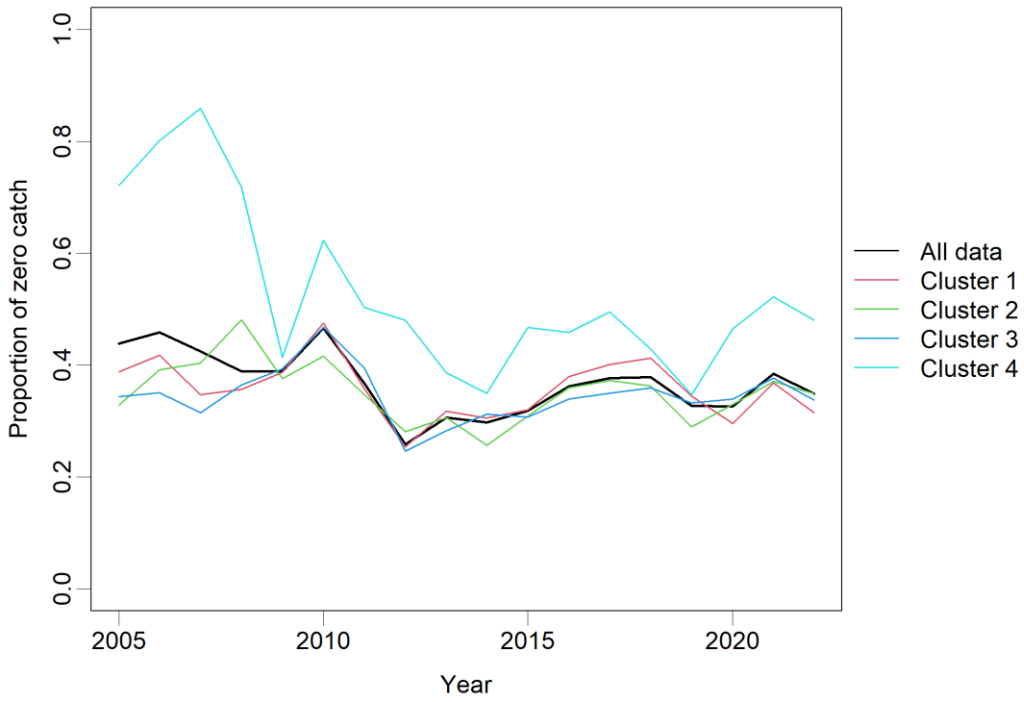

Area NE

Fig. 10. Annual zero proportion of swordfish catches for each cluster of Taiwanese large-scale longline fishery in billfish area of the Indian Ocean.

Area SW

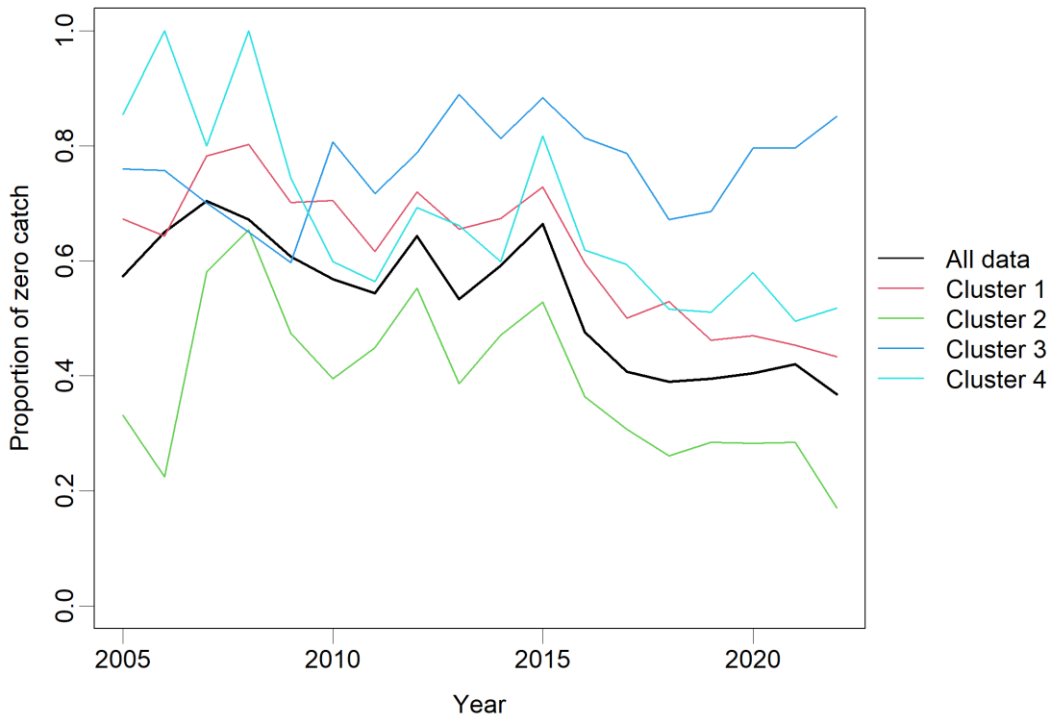

Area SE

Fig. 10. (continued).

Area NW

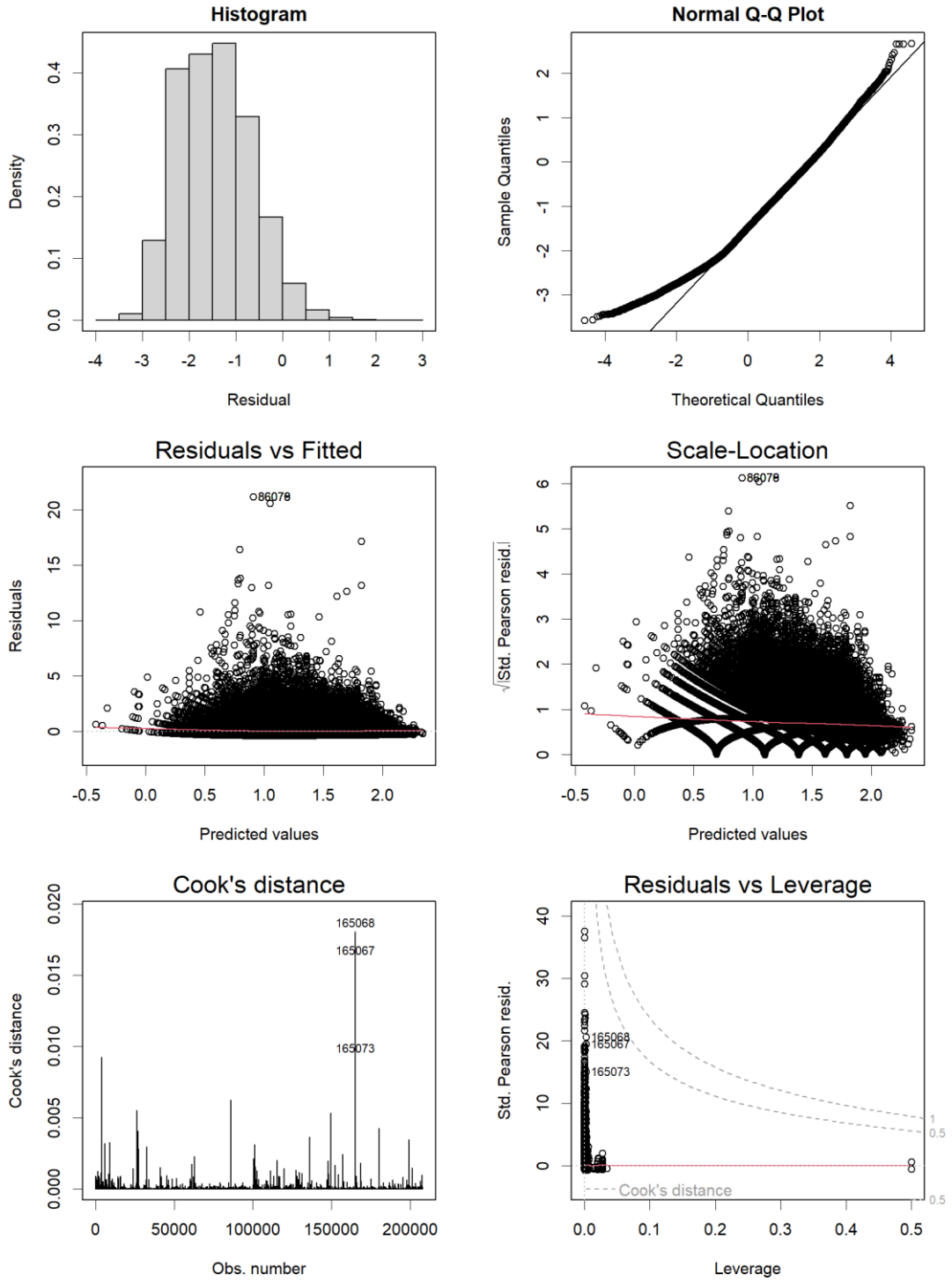

Fig. 11. Diagnostic plots for GLMs with inverse Gaussian error distribution assumption for swordfish caught by Taiwanese large-scale longline fishery in the Indian Ocean from 2005 to 2022.

Area NE

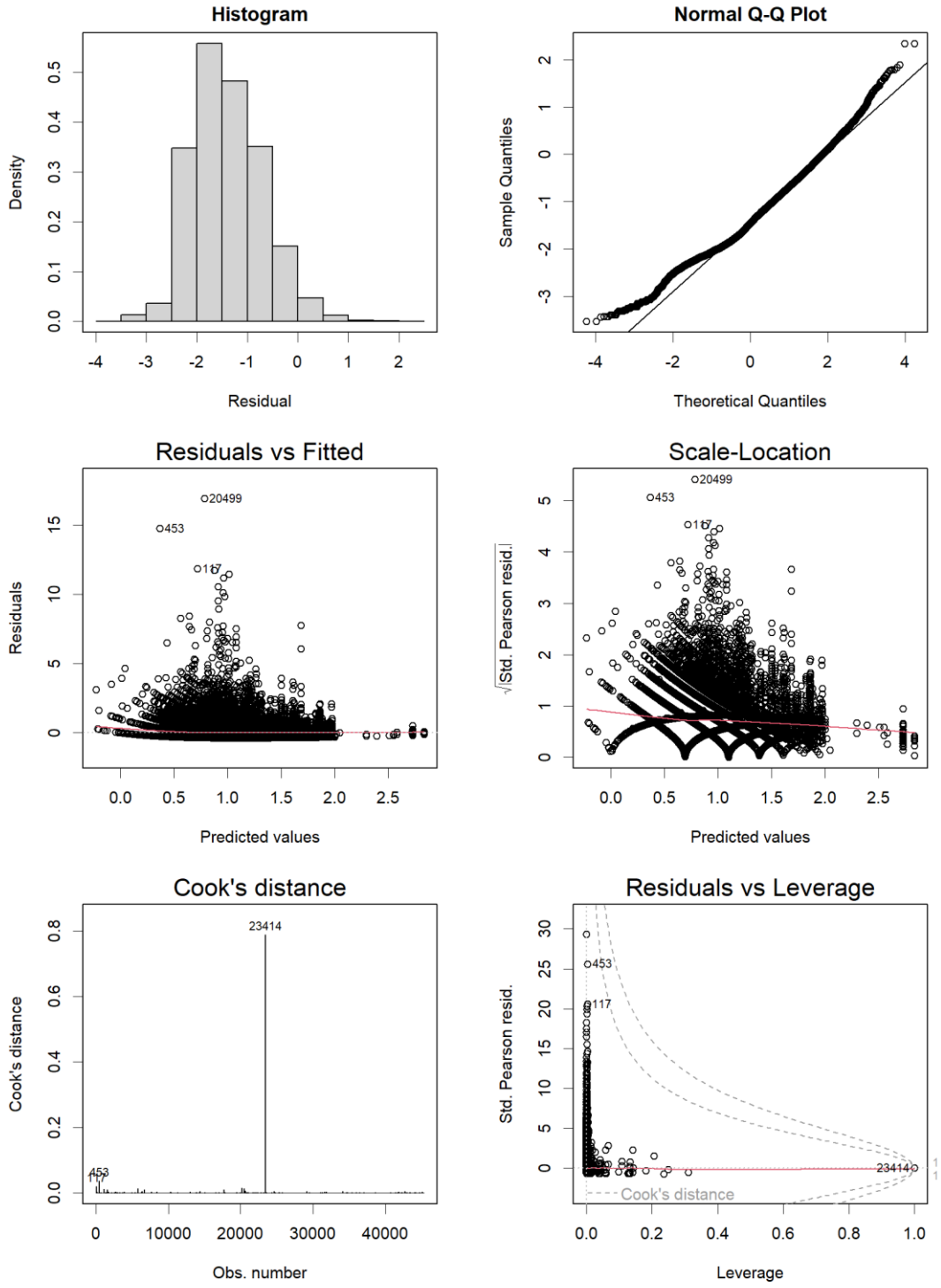

Fig. 11. (continued).

Area SW

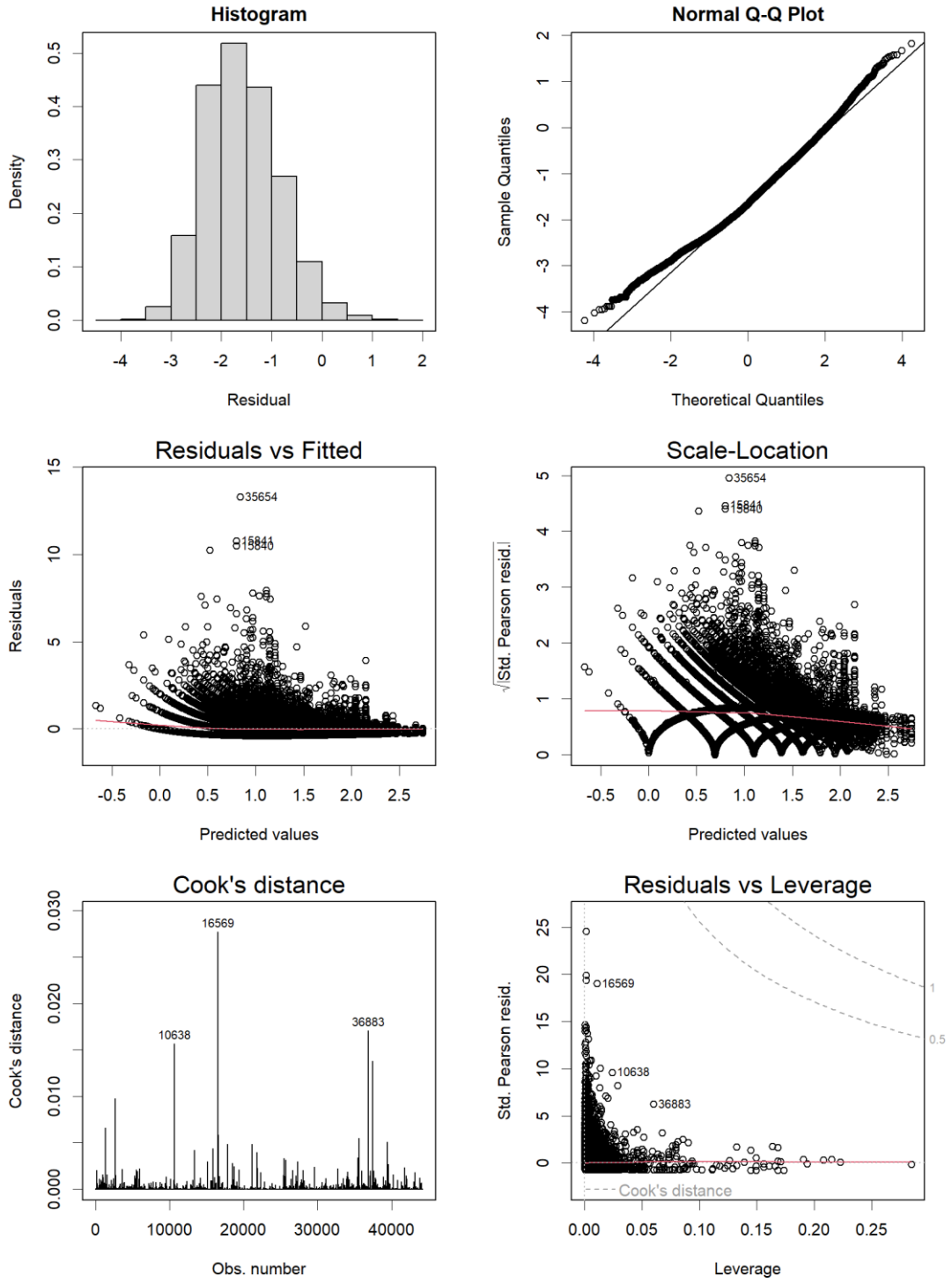

Fig. 11. (continued).

Area SE

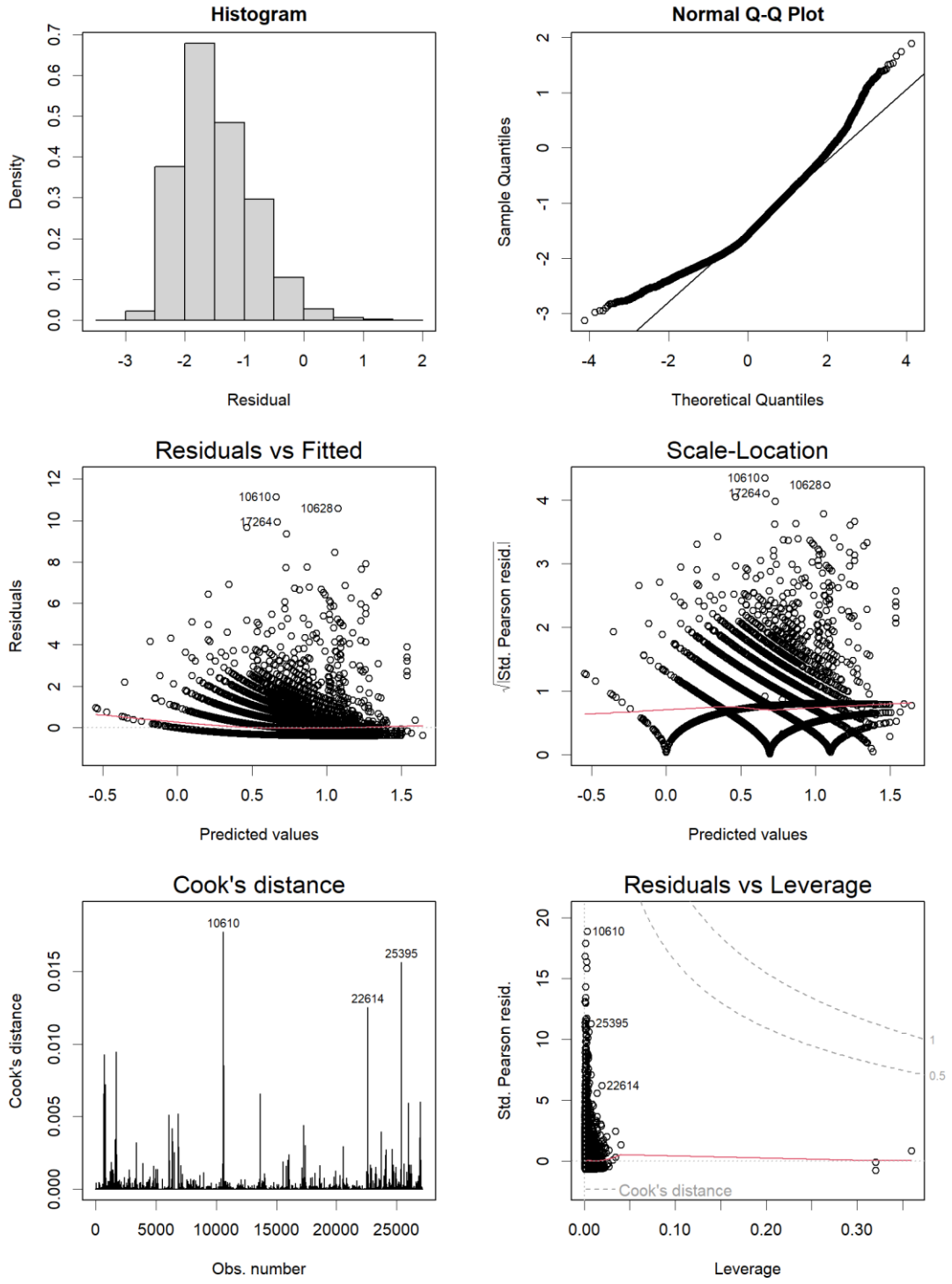

Fig. 11. (continued).

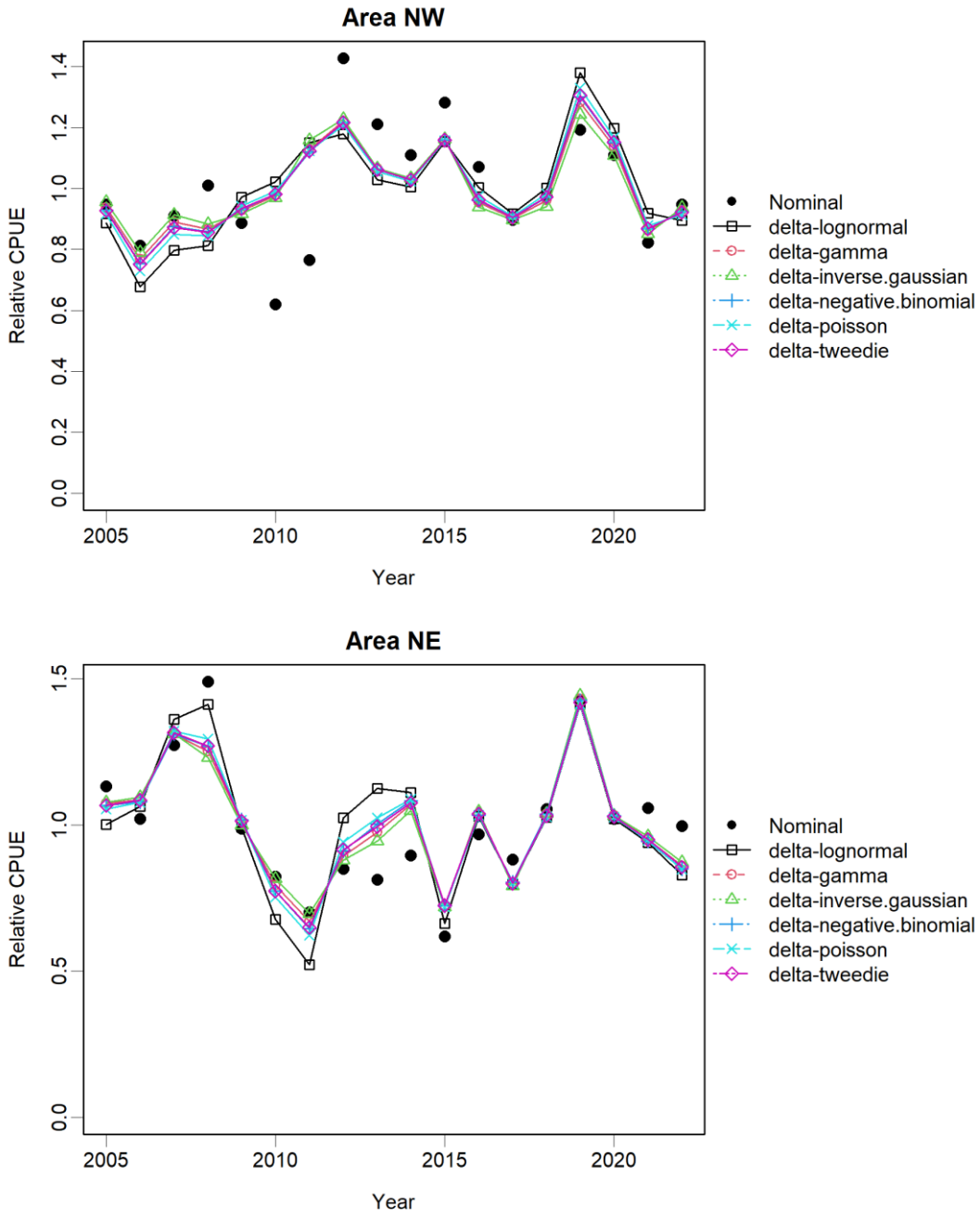

Fig. 12. Standardized CPUE series based on various GLMs for swordfish caught by Taiwanese large-scale longline fishery in the Indian Ocean from 2005 to 2022.

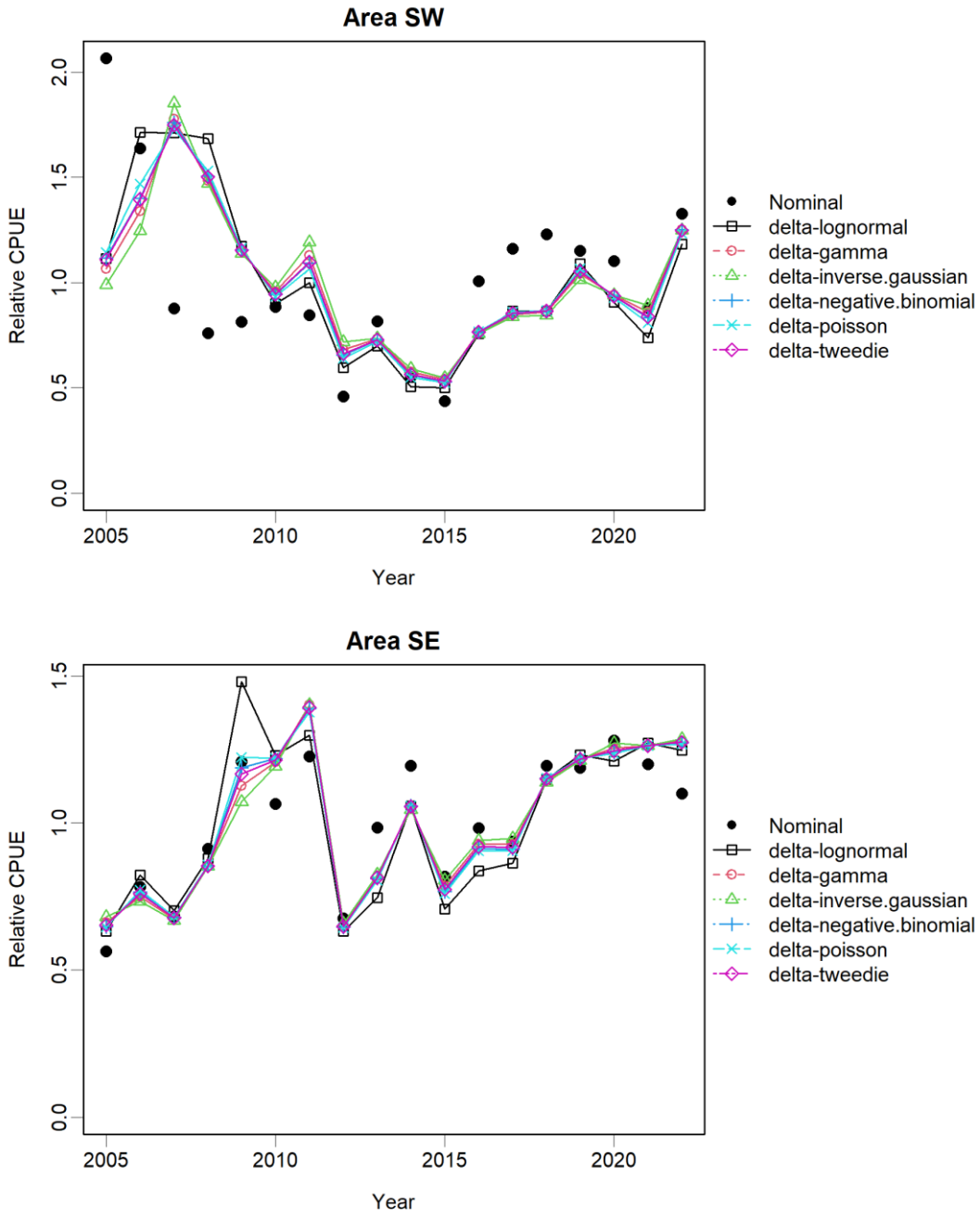

Fig. 12. (continued).

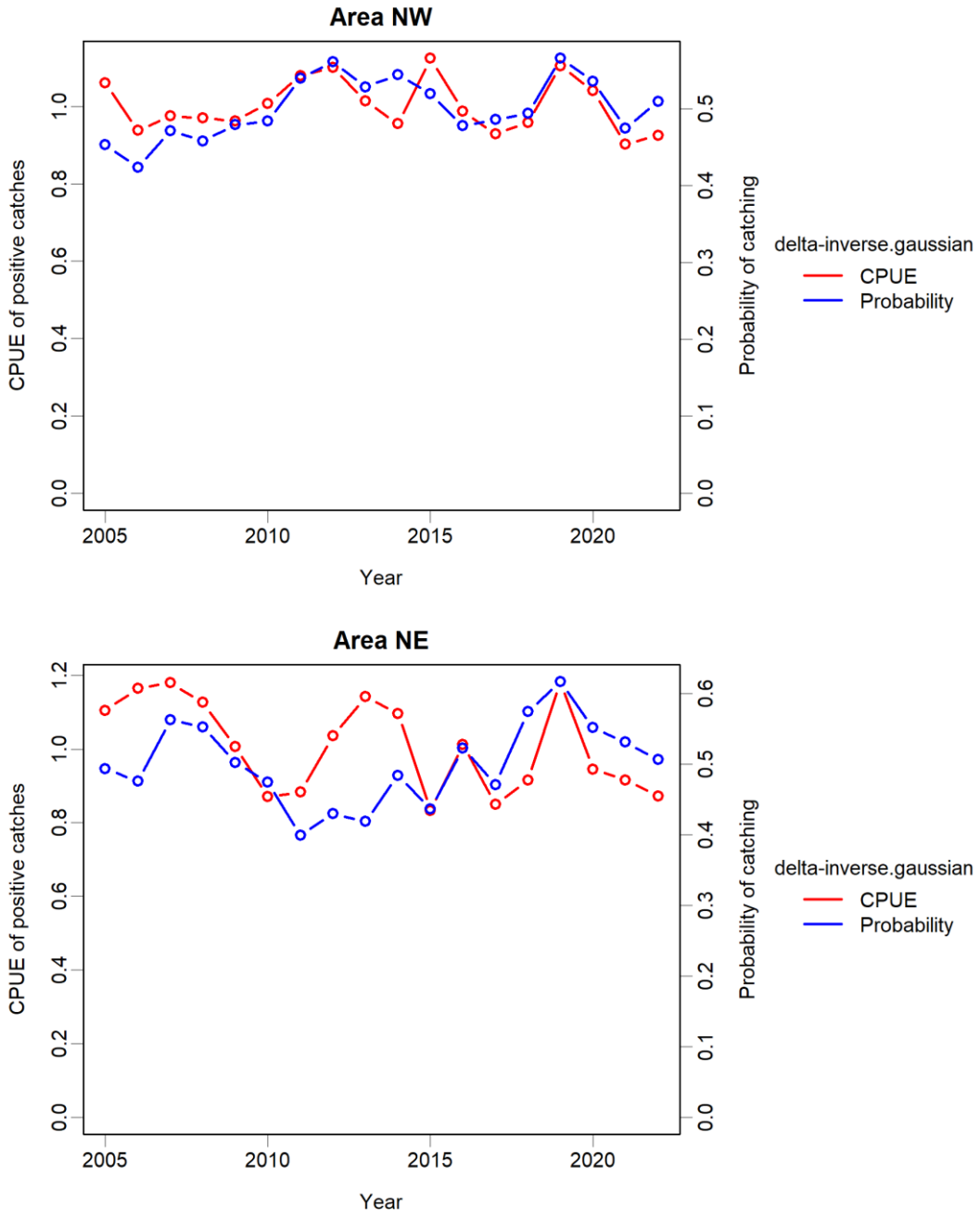

Fig. 13. Standardized CPUE of positive catches and catch probability based on selected model for swordfish caught by Taiwanese large-scale longline fishery in the Indian Ocean from 2005 to 2022.

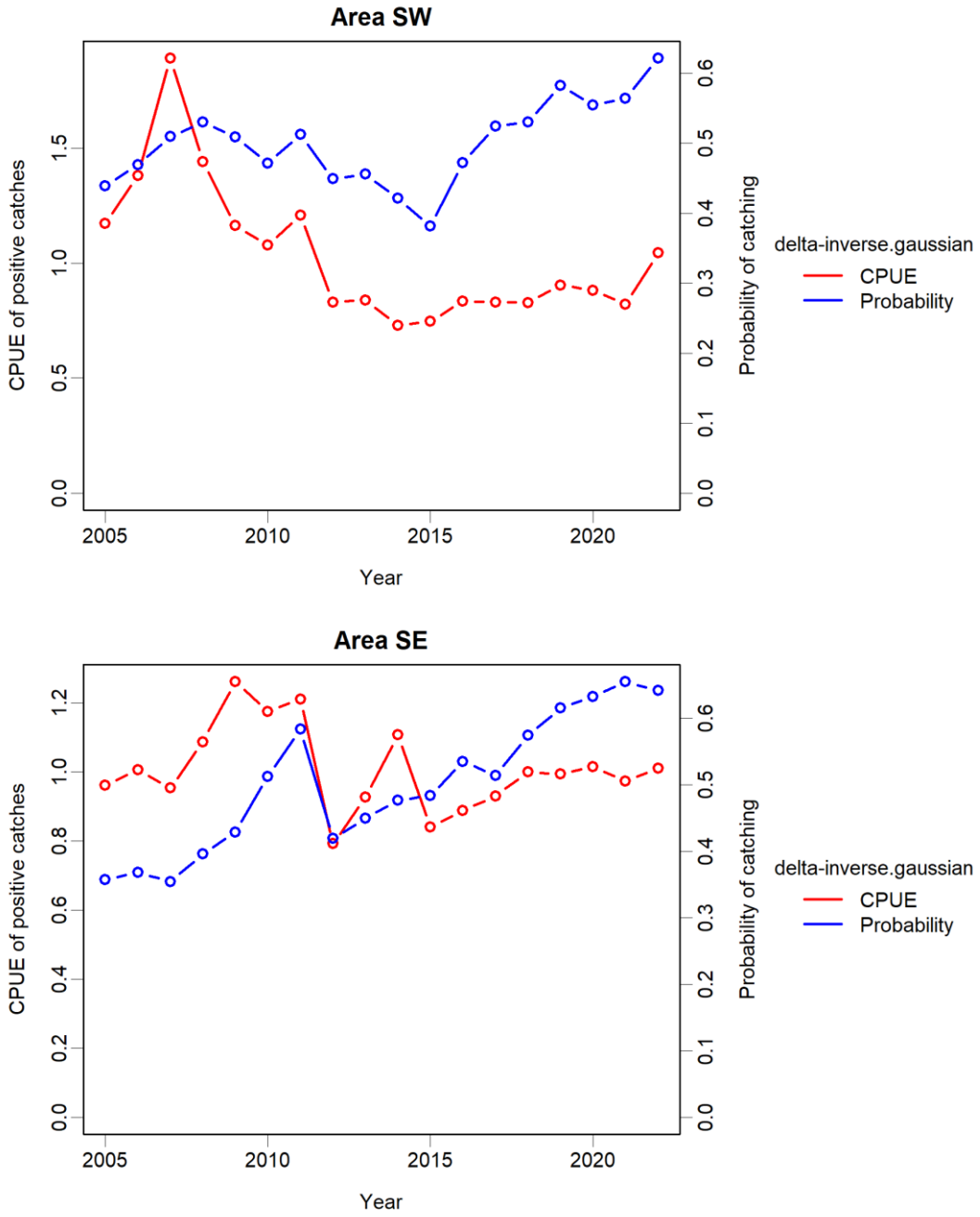

Fig. 13. (continued).

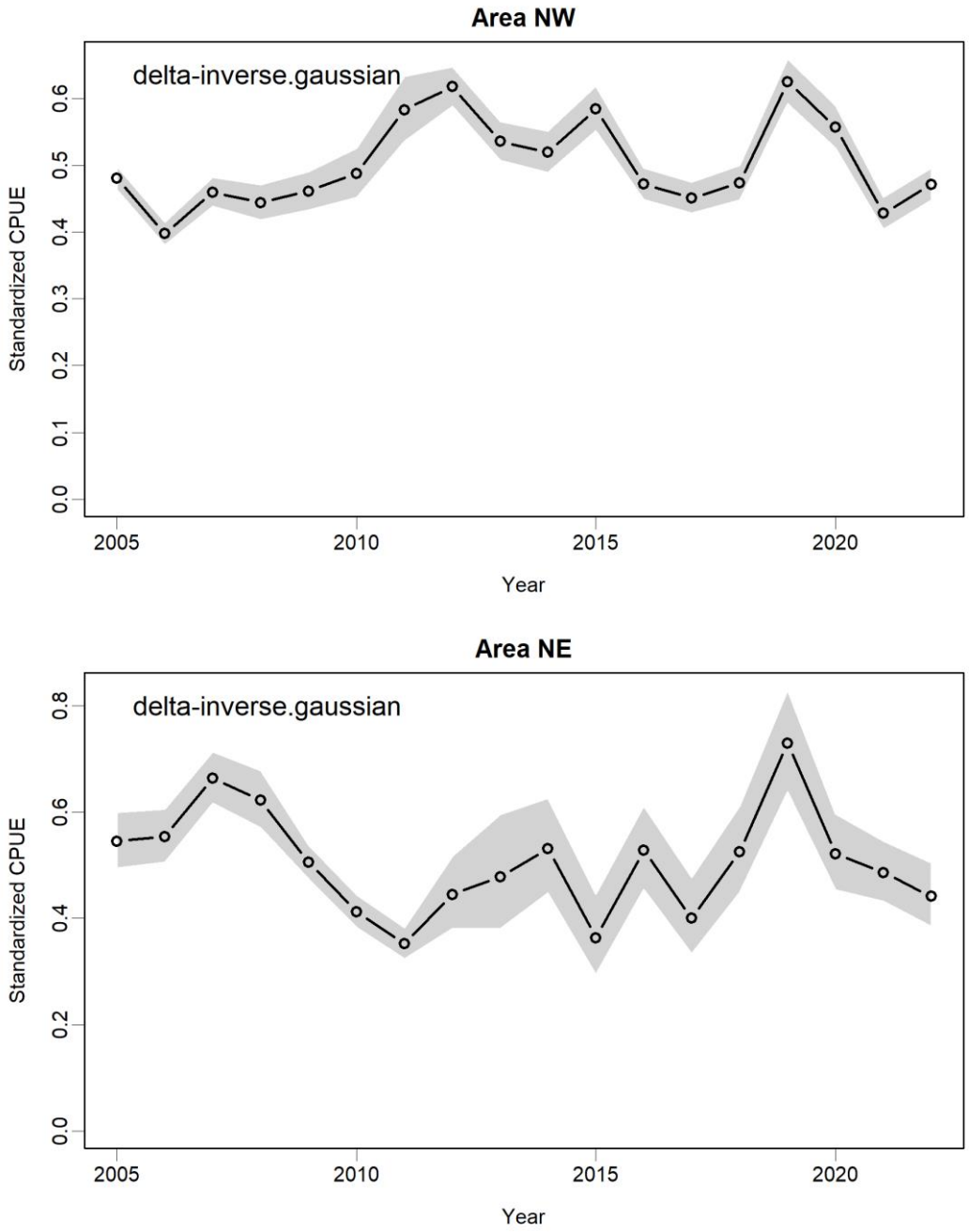

Fig. 14. Standardized CPUE series with 95% confidence intervals based on selected model for swordfish caught by Taiwanese large-scale longline fishery in the Indian Ocean from 2005 to 2022.

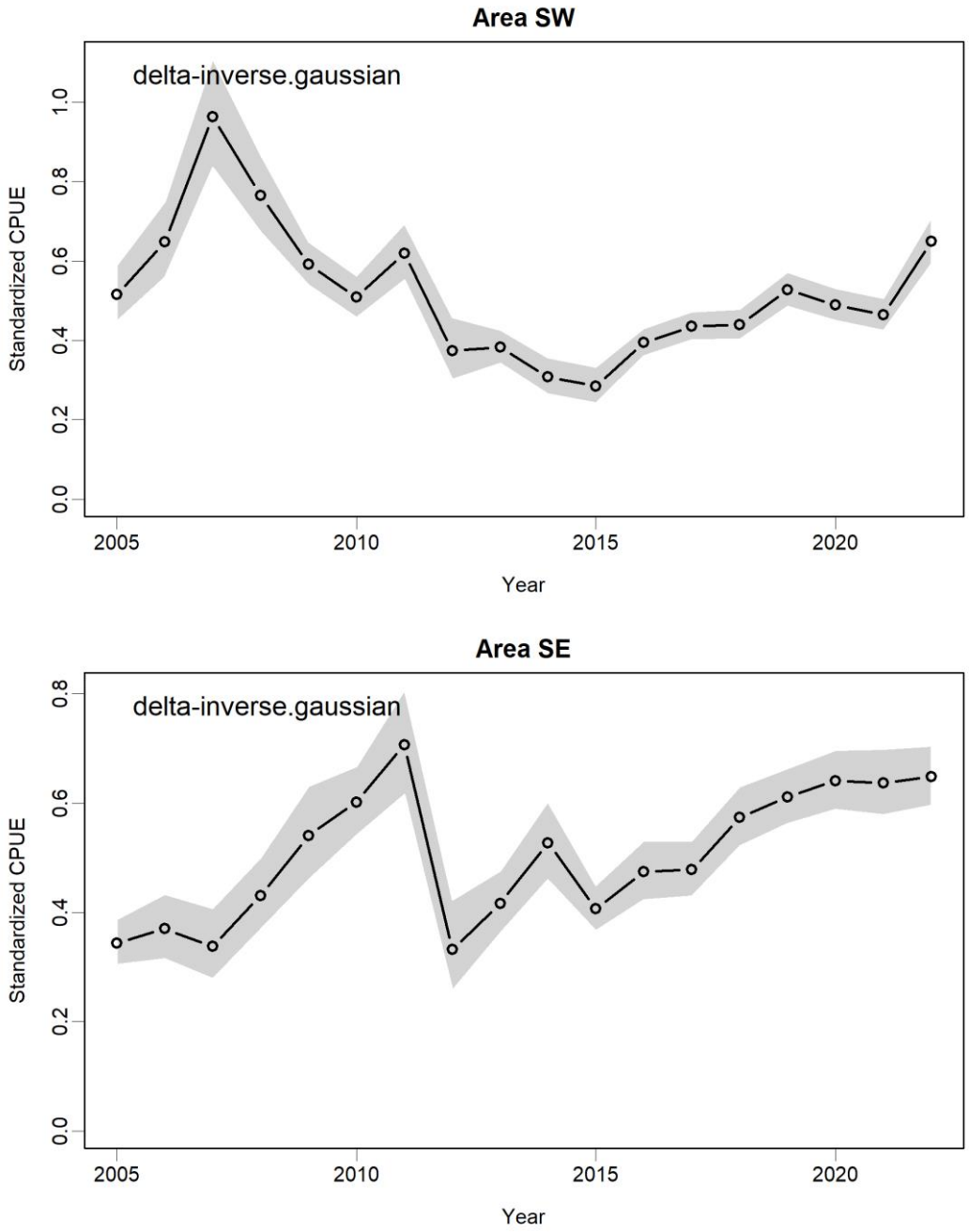

Fig. 14. (continued).

Table 1. Diagnostic statistics for standardized CPUE series based on various models for positive catches of swordfish caught by Taiwanese large-scale longline fishery in the Indian Ocean from 2005 to 2022.

Area	Model	R^2	AIC	BIC
NW	lognormal	0.100	1,171,704	1,172,350
	Gamma	0.152	893,100	893,745
	inverse Gaussian	0.124	839,609	840,254
	tweedie	0.155	949,199	949,845
	Poisson	0.147	1,117,053	1,117,688
	negative binomial	0.160	939,562	940,208
NE	lognormal	0.129	218,667	219,356
	Gamma	0.142	161,958	162,525
	inverse Gaussian	0.118	149,945	150,512
	tweedie	0.151	172,436	173,125
	Poisson	0.151	188,054	188,734
	negative binomial	0.152	176,073	176,640
SW	lognormal	0.248	222,408	223,687
	Gamma	0.323	162,903	164,129
	inverse Gaussian	0.281	151,356	152,634
	tweedie	0.326	173,867	175,145
	Poisson	0.315	192,155	193,425
	negative binomial	0.334	176,552	177,831
SE	lognormal	0.073	116,305	116,806
	Gamma	0.140	78,509	79,009
	inverse Gaussian	0.137	70,007	70,508
	tweedie	0.133	85,042	85,543
	Poisson	0.119	93,265	93,758
	negative binomial	0.130	90,788	91,289

Table 2. ANOVA table for selected standardized CPUE series based on selected GLMs for swordfish caught by Taiwanese large-scale longline fishery in the Indian Ocean from 2005 to 2022.

Area NW

Positive catch model with inverse Gaussian:

	Sum Sq	Df	F values	Pr(>F)
Y	266	17	49.2	< 2.2e-16 ***
Q	59	3	61.3	< 2.2e-16 ***
CT	0	2	0.1	0.9262688
Lon	744	7	334.2	< 2.2e-16 ***
Lat	2290	8	900.3	< 2.2e-16 ***
T	83	3	86.6	< 2.2e-16 ***
Q:CT	19	6	9.8	8.13E-11 ***
Q:T	109	9	38.2	< 2.2e-16 ***
CT:T	8	6	4.3	0.0002254 ***
Residuals	66079	207858		
Signif. codes:	0 ‘***’ 0.001 ‘**’ 0.01 ‘*’ 0.05 ‘.’ 0.1 ‘ ’ 1			

Delta model:

	LR Chisq	Df	Pr(>Chisq)
Y	1724.6	17	< 2.2e-16 ***
Q	40.6	3	7.76E-09 ***
CT	118.9	2	< 2.2e-16 ***
Lon	1830.9	8	< 2.2e-16 ***
Lat	14571	8	< 2.2e-16 ***
T	103	3	< 2.2e-16 ***
hook	326.9	1	< 2.2e-16 ***
Q:CT	90.5	6	< 2.2e-16 ***
Q:T	121.5	9	< 2.2e-16 ***
CT:T	97.3	6	< 2.2e-16 ***
Signif. codes:	0 ‘***’ 0.001 ‘**’ 0.01 ‘*’ 0.05 ‘.’ 0.1 ‘ ’ 1		

Table 2. (continued).

Area NE

Positive catch model with inverse Gaussian:

	Sum Sq	Df	F values	Pr(>F)
Y	225.7	17	39.8	< 2.2e-16 ***
Q	8.8	3	8.8	7.95E-06 ***
Lon	9	6	4.5	0.000148 ***
Lat	154.4	7	66.1	< 2.2e-16 ***
T	73.5	3	73.5	< 2.2e-16 ***
Q:Lon	21.7	18	3.6	3.23E-07 ***
Q:T	38.1	9	12.7	< 2.2e-16 ***
Residuals	15109.4	45282		

Signif. codes: 0 ‘***’ 0.001 ‘**’ 0.01 ‘*’ 0.05 ‘.’ 0.1 ‘ ’ 1

Delta model:

	LR Chisq	Df	Pr(>Chisq)
Y	816.3	17	< 2.2e-16 ***
Q	63.7	3	9.48E-14 ***
CT	76.1	2	< 2.2e-16 ***
Lon	177.7	7	< 2.2e-16 ***
Lat	931.4	7	< 2.2e-16 ***
T	2.9	3	0.4049
hook	60.6	1	6.95E-15 ***
Q:CT	50.0	6	4.64E-09 ***
Q:T	103.7	9	< 2.2e-16 ***
CT:T	76.3	6	2.04E-14 ***

Signif. codes: 0 ‘***’ 0.001 ‘**’ 0.01 ‘*’ 0.05 ‘.’ 0.1 ‘ ’ 1

Table 2. (continued).

Area SW

Positive catch model with inverse Gaussian:

	Sum Sq	Df	F values	Pr(>F)
Y	2171	17	436.1	< 2.2e-16 ***
Q	4	3	4.5	0.003714 **
CT	8	2	13.1	2.01E-06 ***
Lon	8	7	3.9	0.000296 ***
Lat	5	4	4.5	0.001265 **
T	23	3	25.8	< 2.2e-16 ***
Q:CT	4	6	2.4	0.023882 *
Q:Lon	39	21	6.4	< 2.2e-16 ***
Q:Lat	13	12	3.7	1.37E-05 ***
Q:T	29	9	10.9	< 2.2e-16 ***
CT:Lon	25	14	6.2	1.96E-12 ***
CT:Lat	18	8	7.8	1.52E-10 ***
CT:T	49	6	28.0	< 2.2e-16 ***
Lon:T	21	21	3.4	2.27E-07 ***
Lat:T	30	12	8.5	< 2.2e-16 ***
Residuals	12909	44081		

Signif. codes: 0 ‘***’ 0.001 ‘**’ 0.01 ‘*’ 0.05 ‘.’ 0.1 ‘ ’ 1

Table 2. (continued).

Area SW

Delta model:

	LR Chisq	Df	Pr(>Chisq)
Y	712.2	17	< 2.2e-16 ***
Q	12.1	3	0.006976 **
CT	1.1	2	0.588598
Lon	64.5	7	1.90E-11 ***
Lat	36.9	4	1.86E-07 ***
T	116.4	3	< 2.2e-16 ***
hook	99.4	1	< 2.2e-16 ***
Q:CT	57.3	6	1.61E-10 ***
Q:Lon	205.5	21	< 2.2e-16 ***
Q:Lat	230.3	12	< 2.2e-16 ***
Q:T	237.7	9	< 2.2e-16 ***
CT:Lon	101.7	14	2.28E-15 ***
CT:Lat	54.1	8	6.62E-09 ***
CT:T	55.7	6	3.40E-10 ***
Lon:T	222.2	21	< 2.2e-16 ***
Lat:T	420.3	12	< 2.2e-16 ***

Signif. codes: 0 ‘***’ 0.001 ‘**’ 0.01 ‘*’ 0.05 ‘.’ 0.1 ‘ ’ 1

Table 2. (continued).

Area SE

Positive catch model with inverse Gaussian:

	Sum Sq	Df	F values	Pr(>F)
Y	120.8	17	20.4	< 2.2e-16 ***
Q	7.8	3	7.4	5.77E-05 ***
CT	6.2	2	8.8	0.000149 ***
Lon	108.4	10	31.0	< 2.2e-16 ***
Lat	35.6	4	25.5	< 2.2e-16 ***
T	45	3	43.0	< 2.2e-16 ***
Q:CT	14.3	6	6.8	2.93E-07 ***
CT:Lat	15.6	8	5.6	4.03E-07 ***
CT:T	5.9	6	2.8	0.009493 **
Residuals	9455.3	27091		

Signif. codes: 0 ‘***’ 0.001 ‘**’ 0.01 ‘*’ 0.05 ‘.’ 0.1 ‘ ’ 1

Delta model:

	LR Chisq	Df	Pr(>Chisq)
Y	2100.6	17	< 2.2e-16 ***
Q	83.2	3	< 2.2e-16 ***
CT	22.6	2	1.25E-05 ***
Lon	487.9	10	< 2.2e-16 ***
Lat	388.7	4	< 2.2e-16 ***
T	25.6	3	1.16E-05 ***
hook	65.5	1	5.73E-16 ***
Q:CT	43.0	6	1.18E-07 ***
Q:T	23.2	9	0.005802 **
CT:Lat	92.5	8	< 2.2e-16 ***
CT:T	37.4	6	1.44E-06 ***

Signif. codes: 0 ‘***’ 0.001 ‘**’ 0.01 ‘*’ 0.05 ‘.’ 0.1 ‘ ’ 1